Kohn–Sham calculations with the exact functional

Lucas O. Wagner,[1,2,3] Thomas E. Baker,[1] E.M. Stoudenmire,[1,4] Kieron Burke,[2,1] and Steven R. White[1]

[1]*Department of Physics & Astronomy, University of California, Irvine, CA 92697*
[2]*Department of Chemistry, University of California, Irvine, CA 92697*
[3]*Department of Theoretical Chemistry and Amsterdam Center for Multiscale Modeling,*
FEW, Vrije Universiteit, De Boelelaan 1083, 1081HV Amsterdam, The Netherlands
[4]*Perimeter Institute of Theoretical Physics, Waterloo, Ontario, N2L 2Y5, Canada*
(Dated: May 5, 2014)

As a proof of principle, self-consistent Kohn-Sham calculations are performed with the *exact* exchange-correlation functional. The systems calculated are one-dimensional real-space interacting fermions with more than two electrons. To find the exact functional for trial densities requires solving the interacting Schrödinger equation multiple times, a much more demanding task than direct solution of the Schrödinger equation. The density matrix renormalization group method makes this possible. We illustrate and explore the convergence properties of the exact KS scheme for both weakly and strongly correlated systems. We also explore the spin-dependent generalization and densities for which the functional is ill defined.
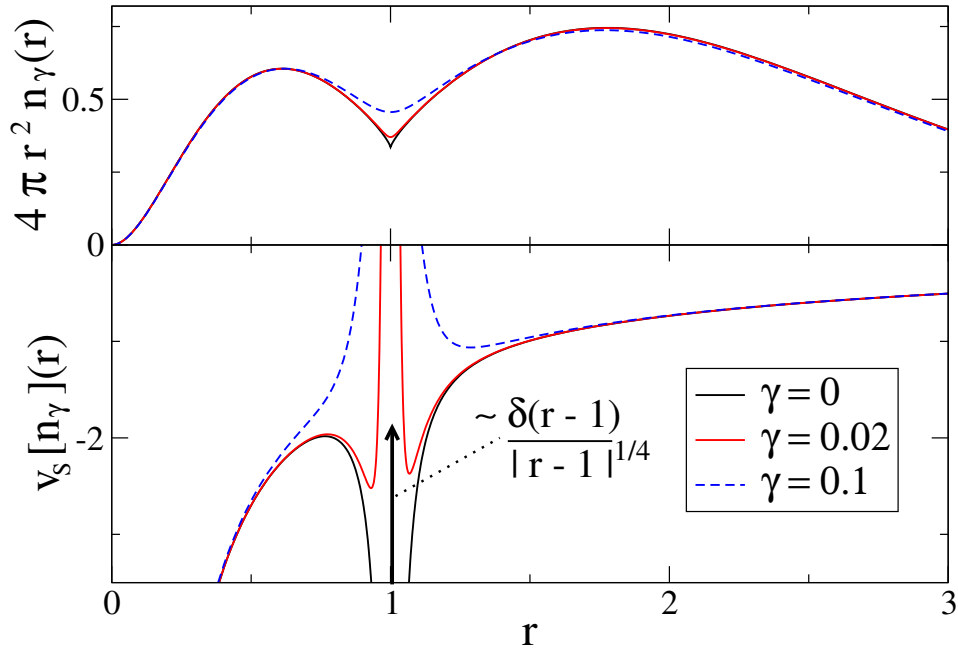
Example of a *reasonable* density (with finite kinetic energy) whose Kohn-Sham potential exists on any grid, but is unphysical in the continuum limit.

PACS numbers: 71.15.Mb, 31.15.E-, 05.10.Cc

CONTENTS

I. INTRODUCTION

Four score and seven years ago, our physics forebears [1, 2] brought into this world a new theory, conceived in simplicity, and dedicated to the proposition that al-

though all particles are waves [3], their density can be simply calculated [1, 2]. Now we are engaged in a great electronic structure debate, testing whether Kohn–Sham theory [4], or any density functional theory [5] so conceived and so dedicated, can endure in the face of strongly correlated systems. We have come to dedicate a portion of this paper, as a final convergence proof [6] for those who have dedicated their lives to developing the constrained search [7] and approximations thereto [8–10]. It is altogether fitting and proper that we should prove this.

Kohn–Sham (KS) [4] density functional theory (DFT) is now a widely used electronic structure method, attaining useful accuracy with present approximations [11]. The method finds the ground-state energy of a many-electron, interacting system by solving an effective non-interacting problem. This non-interacting problem must be solved self-consistently, because its potential (the KS potential) is a functional of the electron density. The most vital piece of this KS potential is derived from the mysterious exchange-correlation functional, which can be computed exactly with great cost [12, 13]. This exact functional provides the formal foundations of KS-DFT for all electronic systems (with some caveats) [7]. However, the utility of KS-DFT derives from simple and computationally efficient approximations to the exchange-correlation (XC) energy [8–10], which can be surprisingly reliable and usefully accurate for broad classes of systems, yet fail badly for others.

Traditionally, study of the exact XC energy functional focussed on finding general exact properties that can either be built into approximations, or used to understand their failures [10, 14–16]. In studying the exact theory we learn what is and is not reproduced by the exact functional; e.g. that the HOMO-LUMO gap of the KS system is not equal to the fundamental (charge) gap of the system [17, 18]. As computational power and algorithms evolved, it also became possible to take a highly accurate solution of the Schrödinger equation, extract the ground-state density, and find the exact KS potential for the system of interest, notably for few electron systems [19–28]. These *inversions* are often quite demanding, since all quantities must be sufficiently accurate to extract the small differences in energies and potentials that form the various components of exchange and correlation.

But even such heroic efforts do *not* produce a way of solving the KS equations with the exact XC functional. This is because, in an actual KS calculation, the XC functional is needed not just for the ground-state density of the system to be solved, but for a sequence of trial densities that ultimately converges to the solution for that problem. To find the XC functional for some trial density, one must solve the Schrödinger equation for the potential for which that density is the ground state, both for interacting and non-interacting electrons. Worse still, these potentials are a priori unknown. Advancing just one step in the KS calculations thus requires solving many interacting electronic problems in order to

find the right potential that yields the trial density. We call this an interacting inversion, and previous examples have been limited to 2 electrons [13, 29, 30].

In this paper, we detail how to find the exact XC functional for realistic models of electrons in one dimension. By realistic, we mean models whose properties mimic those of real systems, and whose treatment with approximate density functionals yields results similar to those for real systems [28]. We use the density matrix renormalization group [31–33] to solve the Schrödinger equation, because of its tremendous efficiency for one-dimensional (1d) systems. In Ref. [6], we used this capability to explore the convergence of a simple algorithm for the KS scheme, ultimately proving that, no matter how strongly correlated, convergence can always be achieved in a finite number of iterations. Various approximate functionals have their own convergence proofs [34, 35], but here we detail exactly how the exact calculations are done, and test further properties of the exact functional.

II. BACKGROUND

Typical solid state and quantum chemistry investigations into electronic structure begin with the non-relativistic continuum Hamiltonian in the Born–Oppenheimer approximation,

$$\hat{H} \equiv \hat{T} + \hat{V} + \hat{V}_{ee} \tag{1}$$
$$\equiv \sum_{i=1}^{N} \left(-\frac{1}{2}\nabla_i^2 + v(\mathbf{r}_i) \right) + \frac{1}{2} \sum_{i \neq j}^{N} \frac{1}{|\mathbf{r}_i - \mathbf{r}_j|},$$

which describes the quantum behavior of N electrons in an external potential $v(\mathbf{r})$ determined by the (classical) nuclei via the operators: the electron kinetic energy $\hat{T}$, their potential energy $\hat{V}$, and the electron-electron interaction $\hat{V}_{ee}$. The eigenstates Ψ_j and eigenvalues E_j (the energies) of the Hamiltonian $\hat{H}$ determine all the properties of the system.

Despite Eq. (1) being the key to everyday electronic structure, an accurate solution for even the ground-state energy E and wavefunction Ψ is not presently tractable for large molecules. This problem continues to inspire the development of new approximations and methods to solve the many-body problem. Some methods—such as Hartree–Fock theory [36], quantum Monte Carlo [37], and coupled cluster [36]—attempt to approximate, sample, or construct the wavefunction. Density functional theory, on the other hand, approaches the many-body problem quite differently.

While Ψ allows one to characterize the system completely, the much simpler ground-state electron density $n(\mathbf{r})$ was proven by Hohenberg and Kohn (HK) to also determine all the properties of the system [5]. Their theorem allows us to formally work with the density as the basic variable instead of the wavefunction [7]. The keystone of this far-reaching proof is the one-to-one correspondence between the ground-state density $n(\mathbf{r})$ and the

potential $v(\mathbf{r})$ of a system, which characterizes the system completely. This one-to-one mapping will be explored in greater detail in Section III, since it is crucial for calculate the exact functional.

As an important mathematical aside, the potential corresponding to a given density is unique if it exists, but there are some densities $n(\mathbf{r})$ which are not *ensemble v-representable,* i.e. not the ground states of any potential $v(\mathbf{r})$ [38]. We explore this complication later, in Section IV G.

A simple corollary of the HK theorem is that the ground-state energy of a system can be determined by minimizing over trial electron densities [5]

$$E_v = \min_n E_v[n] \qquad (2)$$

$$E_v[n] \equiv F[n] + \int d^3r\, n(\mathbf{r})\, v(\mathbf{r}), \qquad (3)$$

where $F[n]$ accounts for the electronic kinetic energy and electron-electron repulsion energy, and is universal, i.e., independent of the external potential $v(\mathbf{r})$. When degeneracy is not an issue [39], the functional $F[n]$ can be found by minimizing the expectation value of $\hat{T} + \hat{V}_{ee}$ over all properly antisymmetric wavefunctions Ψ that yield the density $n(\mathbf{r})$ [7, 12]:

$$F[n] = \min_{\Psi \to n} \langle \Psi | \{ \hat{T} + \hat{V}_{ee} \} | \Psi \rangle, \qquad (4)$$

and the minimizing Ψ is denoted $\Psi[n]$ [40]. The only known way to exactly calculate the functional thus requires use of a wavefunction, albeit implicitly.

We now turn to the formulation of the most popular of DFT implementations, Kohn–Sham DFT [4]. Kohn–Sham theory creates a doppelgänger of the interacting system: a set of non-interacting electrons with the same density. This non-interacting system, the KS system, is characterized by its potential, $v_s[n](\mathbf{r})$, defined implicitly so that a system of N non-interacting electrons in this potential has density $n(\mathbf{r})$. This means that after solving the non-interacting Schrödinger (i.e. KS) equation and obtaining the KS orbitals $\phi_j(\mathbf{r})$ (in Hartree units):

$$\left\{ -\frac{1}{2}\nabla^2 + v_s[n](\mathbf{r}) \right\} \phi_j(\mathbf{r}) = \epsilon_j\, \phi_j(\mathbf{r}). \qquad (5)$$

One finds the density $n(\mathbf{r})$ by occupying the $N/2$ lowest-energy orbitals,

$$n(\mathbf{r}) = 2 \sum_{j=1}^{N/2} |\phi_j(\mathbf{r})|^2 \qquad (6)$$

(where for simplicity we assume that the system is spin-unpolarized). Obtaining the KS potential $v_s[n](\mathbf{r})$ for a density $n(\mathbf{r})$ is an inverse problem, on a firm foundation through the HK theorem applied to non-interacting systems. (Some densities, however, will prove to be non-v-representable [41], so the potential $v_s[n](\mathbf{r})$ is unique, up to a constant, but only if it exists.) Many algorithms

to invert a density to find its KS potential have been suggested [21, 23, 26, 42–45]; ours will be described in Section III.

As a descendent of DFT, Kohn–Sham DFT determines the energy of a system by knowledge of the density alone. Within the KS framework, the universal functional $F[n]$ is written as

$$F[n] = T_s[n] + U[n] + E_{xc}[n] \qquad (7)$$

where $T_s[n]$ is the kinetic energy of the KS orbitals:

$$T_s[n] \equiv -\sum_{j=1}^{N/2} \int d^3r\, \phi_j^*(\mathbf{r})\nabla^2\phi_j(\mathbf{r}), \qquad (8)$$

$U[n]$ is the Hartree energy:

$$U[n] \equiv \frac{1}{2} \int d^3r \int d^3r'\, \frac{n(\mathbf{r})\, n(\mathbf{r}')}{|\mathbf{r} - \mathbf{r}'|}, \qquad (9)$$

and $E_{xc}[n]$ is the exchange-correlation (XC) energy, defined by Eq. (7). Very successful (albeit crude) approximations to $E_{xc}[n]$ have been developed [8–10], which make KS theory a standard and practical approach to electronic structure. Our work focuses on the exact $E_{xc}[n]$, with a few comparisons to the simplest density functional approximation, the local density approximation (LDA) [8].

The KS framework offers a convenient way to minimize $E_v[n]$ as in Eq. (2), by solving non-interacting systems with an effective potential. We guess an input density $n_{in}^{(i)}(\mathbf{r})$ and use it to calculate a trial KS potential $v_s^{(i)}(\mathbf{r})$:

$$v_s^{(i)}(\mathbf{r}) = v(\mathbf{r}) + v_H[n_{in}^{(i)}](\mathbf{r}) + v_{xc}[n_{in}^{(i)}](\mathbf{r}), \qquad (10)$$

where $v_H[n](\mathbf{r}) = \delta U[n]/\delta n(\mathbf{r})$ is the Hartree potential:

$$v_H[n](\mathbf{r}) = \int d^3r'\, \frac{n(\mathbf{r}')}{|\mathbf{r} - \mathbf{r}'|}, \qquad (11)$$

and $v_{xc}[n](\mathbf{r}) = \delta E_{xc}[n]/\delta n(\mathbf{r})$ is the XC potential. The Hartree and XC potentials together account for two-body interactions [46], and are found by taking functional derivatives of their parent energy functionals.

After calculating $v_s^{(i)}(\mathbf{r})$ for the given input density, we solve the trial KS system (i.e. Eq. (5) with our trial KS potential) to obtain an output density $n_{out}^{(i)}(\mathbf{r})$. If the output density equals the input density, we have achieved self-consistency and have found a stationary point of $E_v[n]$. This may be quantified by calculating a simple criterion for convergence:

$$\eta^{(i)} \equiv \frac{1}{N^2} \int d^3r \left(n_{out}^{(i)}(\mathbf{r}) - n_{in}^{(i)}(\mathbf{r}) \right)^2, \qquad (12)$$

declaring the calculation converged when $\eta^{(i)} < \delta$, If the calculation has not converged, a new guess density $n_{in}^{(i+1)}(\mathbf{r})$, such as $n_{out}^{(i)}(\mathbf{r})$, is plugged into Eq. (10) for

the next iteration, and we repeat until converged. For the exact XC functional, the converged density is the ground-state density of interacting electrons in the potential $v(\mathbf{r})$ [6]. This iterative-convergence procedure is known as the KS scheme [47], and is illustrated in Fig. 1. The possibility of finding other stationary points besides the ground-state for the exact functional will be addressed in Section IV.

The Kohn–Sham DFT approach to electronic structure thus converts the many-body problem into a non-interacting problem which must be solved self-consistently. The exact procedure requires finding the many-body system with a given density, with wavefunction $\Psi[n]$, to determine $E_{\mathrm{XC}}[n]$ and $v_{\mathrm{XC}}[n](\mathbf{r})$, and thus is as costly as solving the original many-body problem (see Section IV). However, the KS scheme would be neither useful nor practical at such a computational cost. Evaluating $v_{\mathrm{XC}}[n](\mathbf{r})$ at each iteration of the KS scheme is (usually) a trivial and inexpensive step with present approximations, since the functional derivative is known explicitly.

III.   INVERSIONS

Inverting a density $n(\mathbf{r})$ to find its KS potential $v_{\mathrm{S}}[n](\mathbf{r})$, or to find its external potential $v[n](\mathbf{r})$ (for real, interacting electrons) is not a straightforward task. In this section we discuss how to do this for an arbitrary v-representable density. As a by-product of these inversions, we obtain the implicitly defined KS orbitals and interacting wavefunction $\Psi[n]$, which allow us to evaluate the XC potential and energy in Section IV.

Non-interacting inversions are performed to find the KS potential of exact densities for a variety of systems [20, 28, 48]. The notation we use for the potential corresponding to the density $n(\mathbf{r})$ of non-interacting electrons

is $v_{\mathrm{S}}[n](\mathbf{r})$, which we have already seen in Eq. (5). This inversion is a simple matter for one or two electrons with opposite spins, since the KS equation can be rearranged to obtain:

$$v_{\mathrm{S}}[n](\mathbf{r}) = \frac{1}{2} \frac{\nabla^2 \sqrt{n(\mathbf{r})}}{\sqrt{n(\mathbf{r})}} + \epsilon, \quad (N \leq 2) \qquad (13)$$

where ϵ is a constant (the only occupied KS eigenvalue). For more electrons, one can use an iterative procedure to determine $v_{\mathrm{S}}[n](\mathbf{r})$. Initially a potential $v_{\mathrm{S}}^{(1)}(\mathbf{r})$ is guessed, e.g. Eq. (13). Then, starting with $i = 1$:

1. For the potential $v_{\mathrm{S}}^{(i)}(\mathbf{r})$, solve the non-interacting Schrödinger equation for orbitals $\phi_j^{(i)}(\mathbf{r})$, doubly-occupying to obtain the density $n^{(i)}(\mathbf{r})$.

2. If $n^{(i)}(\mathbf{r})$ is within tolerance of $n(\mathbf{r})$, we are done, i.e. $v_{\mathrm{S}}^{(i)}(\mathbf{r}) = v_{\mathrm{S}}[n](\mathbf{r})$ and $\phi_j(\mathbf{r}) = \phi_j^{(i)}(\mathbf{r})$. Otherwise, continue.

3. A new potential $v_{\mathrm{S}}^{(i+1)}(\mathbf{r})$ is chosen, based on how different $n^{(i)}(\mathbf{r})$ is from $n(\mathbf{r})$. Roughly speaking, where $n^{(i)}(\mathbf{r})$ is too low, the new potential $v_{\mathrm{S}}^{(i+1)}(\mathbf{r})$ is lowered from the old $v_{\mathrm{S}}^{(i)}(\mathbf{r})$, and where $n^{(i)}(\mathbf{r})$ is too high, the new potential is raised.

4. Increment i and repeat steps 1 to 4.

The only difference between different inversion algorithms is how the new potential is determined in step 3. The problem can be reduced to finding the root of a non-linear function of many variables, which can be treated at various levels of sophistication [49]. We discuss Broyden's method at the end of this section. With the KS potential $v_{\mathrm{S}}[n](\mathbf{r})$ and orbitals $\phi_j(\mathbf{r})$, we can evaluate functionals such as $T_{\mathrm{S}}[n]$ using Eq. (8).

Interacting inversions are rarely done, since they are far more expensive than non-interacting inversions, and require solving the many-body problem many times. Only two-electron problems have been studied, in one case to understand the adiabatic approximation within TDDFT [29, 30] and in another to study the self-interaction error within LDA [13]; though we have recently studied four-electron systems [6]. The potential $v[n](\mathbf{r})$, which corresponds to the interacting system of electrons with density $n(\mathbf{r})$, can be found using the same algorithm as for $v_{\mathrm{S}}[n](\mathbf{r})$, though in step 1 we must solve an interacting problem for the many-body wavefunction $\Psi^{(i)}$ rather than the non-interacting Schrödinger equation for orbitals $\phi_j^{(i)}(\mathbf{r})$. At the end of the inversion we obtain $\Psi[n]$, the wavefunction which minimizes $F[n]$ in Eq. (4), allowing us to compute $F[n]$ for that specific density.

To illustrate the theory behind KS-DFT, we solve interacting systems using the density matrix renormalization group (DMRG) [31, 32], which is the most efficient wavefunction solver in 1d, capable of handling both
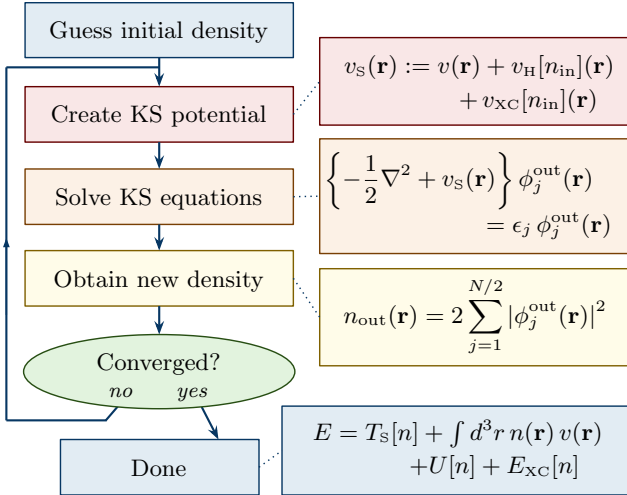

FIG. 1. The KS scheme.

Guess initial density

Create KS potential

$v_{\mathrm{S}}(\mathbf{r}) := v(\mathbf{r}) + v_{\mathrm{H}}[n_{\mathrm{in}}](\mathbf{r})$
$+ v_{\mathrm{XC}}[n_{\mathrm{in}}](\mathbf{r})$

Solve KS equations

$\left\{ -\frac{1}{2}\nabla^2 + v_{\mathrm{S}}(\mathbf{r}) \right\} \phi_j^{\mathrm{out}}(\mathbf{r})$
$= \epsilon_j \, \phi_j^{\mathrm{out}}(\mathbf{r})$

Obtain new density

$n_{\mathrm{out}}(\mathbf{r}) = 2 \sum_{j=1}^{N/2} |\phi_j^{\mathrm{out}}(\mathbf{r})|^2$

Converged?
no   *yes*

Done

$E = T_{\mathrm{S}}[n] + \int d^3r \, n(\mathbf{r})\, v(\mathbf{r})$
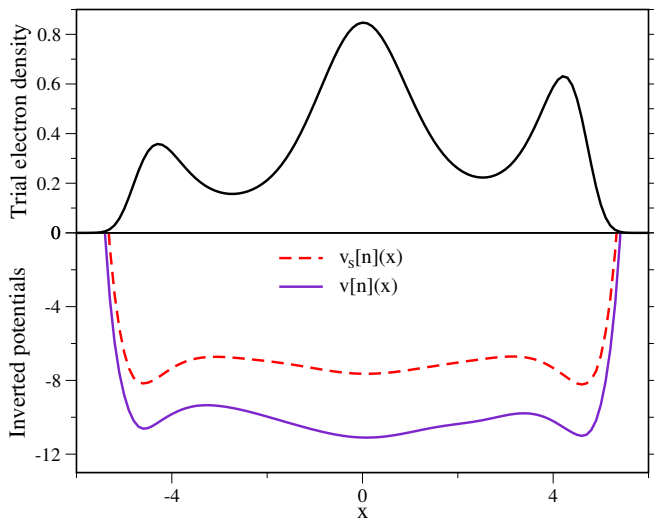$+ U[n] + E_{\mathrm{XC}}[n]$

FIG. 2. Density inversion of arbitrary 4-electron density for non-interacting and interacting potentials.

strong and weak correlation. We apply DMRG to model 1d continuum systems by discretizing space into N_g grid points with a small grid spacing Δ [28, 50]. With this method, we can invert 1d systems with over 100 electrons [50]. For our model systems we employ a softened Coulomb interaction between electrons [28, 29, 50–52]:

$$v_{\text{ee}}(u) = 1/\sqrt{u^2 + 1}. \tag{14}$$

Figure 2 shows a four-electron example of an interacting inversion [53]. For some arbitrary density like this one (meaning a density we would not find in nature), we want to find the associated KS and interacting potentials. This is the problem we encounter during the self-consistent calculation of the KS equations. Since we ultimately find $\Psi[n]$ at the end of the inversion, we can evaluate $F[n]$ (given soft-Coulomb interactions); likewise with $\phi_j(\mathbf{r})$ we can obtain $T_{\text{s}}[n]$. For the example density of Fig. 2 we find $F[n] = 3.07$, $T_{\text{s}}[n] = 0.843$, $U[n] = 3.628$, so $E_{\text{xc}}[n] = -1.397$. The XC energy is thus calculated using simple energy differences; and we obtain the XC potential in the same way. We further describe these matters in the next section.

To close this section, we describe our recipe for step 3 of the inversion algorithm. The idea is to build an approximation for the density-density response matrix, χ, which determines how a small change in the potential will change the density:

$$\int d^3r' \, \chi(\mathbf{r}, \mathbf{r}') \, \delta v(\mathbf{r}') = \delta n(\mathbf{r}). \tag{15}$$

Restricting our attention to 1d, we recast this equation as the matrix equation $\chi \delta v = \delta n$, where χ is an (unknown) $N_g \times N_g$ matrix, and δv, δn are vectors with N_g components, where N_g is the number of grid-sites in the system. A constant change in the potential (i.e. $\delta v = c_1$) will give zero change in the density ($\delta n = 0$),

and a constant change in the density ($\delta n = c_2$) is impossible, since N is fixed. Therefore we consider orthonormal basis functions for changes in the potential and density which integrate to zero, encoded as columns in the matrices W and M, respectively [54]. Within this basis, the density-density response matrix can be approximated by a smaller matrix, A:

$$\chi \approx MAW^T. \tag{16}$$

This factorization of the matrix χ looks very much like (and is inspired by) the singular value decomposition (SVD) of χ, which would give an exact breakdown of χ into optimal bases M and W, with A being diagonal. We do not know χ a priori, but an approximation to χ (or A) can be iteratively improved using a quasi-Newton method (we use Broyden's method [55]). We construct appropriate basis vectors for M and W using orthonormalized differences of trial densities from the target density. As A is refined, the bases M and W can be optimized (if desired) by computing the SVD of A, a procedure which is also useful to compute A^{-1}, and thus χ^{-1}. The next trial potential for step 3 is determined by: $v^{(i+1)} = v^{(i)} + \chi^{-1}(n - n^{(i)})$. Typically around 20 basis vectors in M and W are required to obtain a trial density indistinguishable from the target density on the scale of Fig. 2.

IV. RESULTS

We have now sufficient machinery to calculate the exact exchange-correlation energy and potential for any trial density, as encountered in the KS scheme. For convenience, we define $E_{\text{HXC}}[n] \equiv U[n] + E_{\text{XC}}[n]$, which can be evaluated (using Eqs. (4) and (7)) as:

$$E_{\text{HXC}}[n] = \langle \Psi[n]|\{\hat{T} + \hat{V}_{\text{ee}}\}|\Psi[n]\rangle - T_{\text{s}}[n]. \tag{17}$$

From Section III, we know how to obtain $\Psi[n]$ and $T_{\text{s}}[n]$ using inversions. Therefore the exact $E_{\text{xc}}[n]$ is no obstacle in principle, but extremely computationally expensive in practice. Similarly, the HXC potential is:

$$v_{\text{HXC}}[n](\mathbf{r}) = v_{\text{s}}[n](\mathbf{r}) - v[n](\mathbf{r}), \tag{18}$$

which are available from interacting and non-interacting inversions. The construction of the exact functional using inversions is illustrated in Fig. 3.

To algorithmically implement the KS scheme, we must choose our input densities $n_{\text{in}}^{(i)}(\mathbf{r})$ for each iteration i; each output density $n_{\text{out}}^{(i)}(\mathbf{r})$ is determined by solving the KS equations (5). Although more sophisticated algorithms are used in practice [34, 57–62], we choose the simple algorithm given below. We emphasize that we make no claims as to the efficiency of this particular algorithm. We expect many other algoritms to be more efficient. But this simple choice allows a simple proof of convergence,

and provides an initial framework to study convergence rate questions.

The first input density $n_{\text{in}}^{(1)}(\mathbf{r})$ is arbitrarily chosen. The subsequent input densities are calculated via the linear density mixing algorithm,

$$n_{\text{in}}^{(i+1)}(\mathbf{r}) = (1 - \lambda)\, n_{\text{in}}^{(i)}(\mathbf{r}) + \lambda\, n_{\text{out}}^{(i)}(\mathbf{r}), \qquad (19)$$

where λ is a parameter between 0 and 1, which aids convergence. At $\lambda = 1$, no density mixing is performed, and the output density of iteration i is used as the input for iteration $i + 1$. While this might allow for quick convergence, there is the danger of repeatedly overshooting the ground-state density and not converging. If this happens, smaller steps must be taken, i.e. small λ ($\lambda = 0$ not allowed) must be used. These convergence issues are discussed more thoroughly in Section IV B, where we investigate how small this density mixing λ needs to be in order to converge the calculation.

A. Illustration

In this section we use the exact functional within the KS scheme for a model one-dimensional continuum system, demonstrating convergence to the true ground-state density. We also explain why the only stationary point of the exact functional is the true ground-state density.

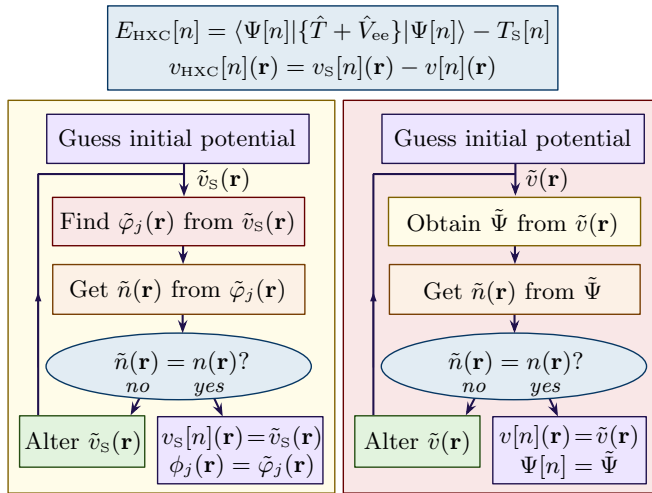In our model one-dimensional system, electrons are at-

FIG. 3. To determine the $E_{\text{HXC}}[n]$ and $v_{\text{HXC}}[n](\mathbf{r})$: Our exact calculation requires a computationally demanding inversion algorithm to find the one-body potential $v[n](\mathbf{r})$ of the interacting system whose density is $n(\mathbf{r})$, with KS orbitals $\phi(\mathbf{r})$, in addition to a non-interacting inversion to find $v_{\text{S}}[n](\mathbf{r})$. In case of degeneracy, mixed-states should be used instead of pure-state wavefunctions in both non-interacting and interacting inversions [7, 56]. The right hand side differs from the left in that it describes an interacting inversion.
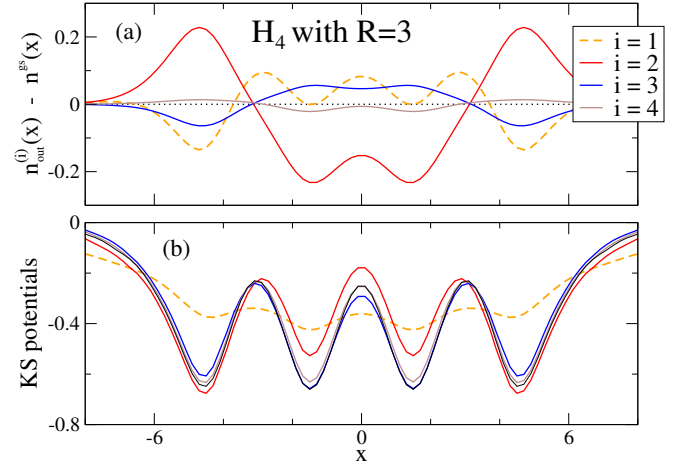

FIG. 4. KS procedure for a moderately correlated 4-electron system (four hydrogen atoms separated by an interatomic spacing of $R = 3$), using a fixed $\lambda = 0.3$ and showing the first few iterations of: (a) differences in the trial output densities from the ground-state density (shown in Fig. 5) and (b) trial KS potentials. Data from Ref. [6].

tracted to the nuclei via the potential [28]

$$v_{\text{e-nuc}}(x) = -1/\sqrt{x^2 + 1}, \qquad (20)$$

and electrons interact with the corresponding repulsive potential as already mentioned via Eq. (14).

In Fig. 4, we plot the trial densities and KS potentials for a four-electron, four-atom system. The interatomic spacing R is chosen to make correlations moderate. Choosing a density mixing of $\lambda = 0.30$ affords fairly rapid convergence. We find that the final density, calculated within our KS algorithm, is equal to the true ground-state density of the system. We plot the final converged KS, Hartree, and XC potentials in Fig. 5.

Regarding stationary points of the exact functional, we find that, in all the cases we ran, our KS algorithm converged to the true ground-state density. An analytic result confirms that, given v-representable densities, the only stationary point of the exact KS scheme is the ground-state density of the system [63]. We can see this by plugging the exact $v_{\text{HXC}}[n](\mathbf{r})$ from Eq. (18) into the KS update (10). The exact scheme then proceeds as

$$v_{\text{S}}(\mathbf{r}) := v_{\text{S}}[n_{\text{in}}](\mathbf{r}) + \big(v(\mathbf{r}) - v[n_{\text{in}}](\mathbf{r})\big), \qquad (21)$$

with self-consistency reached when $v(\mathbf{r}) = v[n_{\text{in}}](\mathbf{r})$. This occurs at precisely one density: at the ground-state density $n^{\text{gs}}(\mathbf{r})$, which is unique by the HK theorem. Thus the exact KS scheme has only one stationary point for v-representable densities.

In density functional theory, there is no guarantee that a KS potential exists for a given physical system. The guarantee is that if it does exist, it is unique and, as we pointed out above, the only stationary point of the KS equations. Densities with legitimate KS potentials are called non-interacting v-representable. We
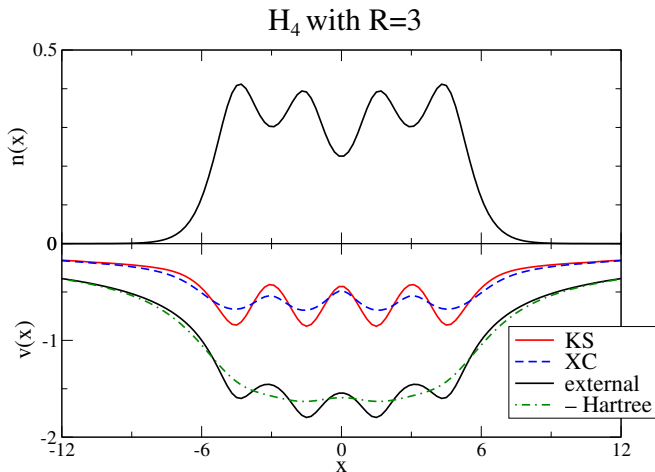
FIG. 5. External, KS, Hartree, and XC potentials, as well as the ground-state density, for a moderately correlated 4-electron system (four hydrogen atoms separated by an interatomic spacing of $R = 3$).

have performed many non-interacting inversions on accurate ground-state densities of atomic chains, and have always found their KS potentials to exist, even when the bond lengths are stretched. Since standard density functional approximations usually become inaccurate for strongly correlated systems, such as when bonds are stretched, a potential pitfall for KS-DFT is that such systems may fail to be non-interacting v-representable. While there are subtleties to identifying whether a density is v-representable or not (as discussed further in Section IV G), v-representability does not appear to be the main issue when strong correlation is involved [64–67]. Instead, good approximate functionals simply are missing at present [68, 69]. If v-representability were to blame, the entire KS apparatus, despite being exact in principle, could not be applied to such systems. Happily, our results show no evidence of such a disastrous situation.

B. First steps

Knowing that there is only one stationary point of the KS scheme (for v-representable densities) tells us nothing about the difficulty in finding it. In this section we consider the most basic part of the KS scheme – a single step in the KS algorithm – which will help us understand the convergence behavior of the exact functional for different systems. We will see why strongly correlated systems are more difficult to converge than weakly correlated systems.

To explore how the KS scheme converges, we calculate the energy of the system which interpolates between the input and output densities for a single step of the algorithm, measured against the ground-state energy:

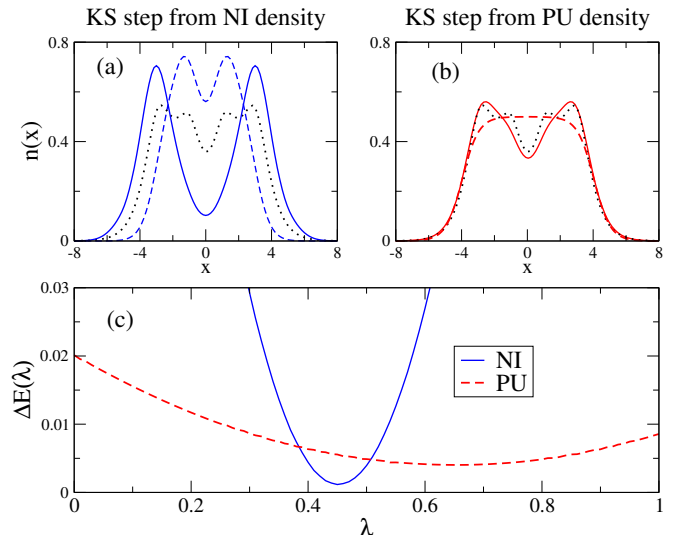$$\Delta E(\lambda) = E_v[n_\lambda] - E_v, \qquad (22)$$

FIG. 6. A single step in the KS scheme for a weakly correlated system (H_4 with $R = 2$) away from two different initial densities: non-interacting electrons in the external potential (NI) and a pseudouniform electron density (PU). These initial densities are the dashed curves in (a) and (b), and the solid curves are the output densities for each KS step; for comparison the dotted curve is the exact density. The lower panel plots Eq. (22), the energy of the system as it interpolates from the input to the output density.

where $n_\lambda(\mathbf{r})$ linearly interpolates between the input density (at $\lambda = 0$) to the output density ($\lambda = 1$), just as in Eq. (19). We plot $\Delta E(\lambda)$ as well as the input, output, and exact densities for various systems in Figures 6 and 7. As can be seen, the output density is in the right direction to minimize $E_v[n]$, but it overshoots the minimum. Starting the next iteration of the KS scheme with this output density would not (in general) allow convergence; therefore a mixture of the input and output densities is used as the next input, thus motivating Eq. (19). The optimal mixing λ minimizes $E_v[n_\lambda]$ on the interval $(0, 1]$, and could be found using a line search. But even with the optimal mixing, neither of the chosen starting points (a non-interacting and a pseudouniform density) produces the ground-state density on the first iteration, so it takes a few iterations to converge. It is perhaps surprising, however, that a single iteration of the KS scheme could get so close to the ground state. For the weakly correlated system (Fig. 6), the non-interacting starting point gets within $\Delta E = 0.001$ of the ground-state energy with $\lambda = 0.45$, whereas the pseudouniform starting point minimizes $\Delta E = 0.004$ with $\lambda = 0.45$. For the strongly correlated system (Fig. 7), the optimal λ's are smaller and the ΔE's are larger: the non-interacting initial point minimizes at $\Delta E = 0.002$ with $\lambda = 0.44$, and the pseudouniform initial point minimizes ΔE at 0.094 around $\lambda = 0.21$.

Figures 6 and 7 each plot only two cuts through the infinite-dimensional functional landscape.

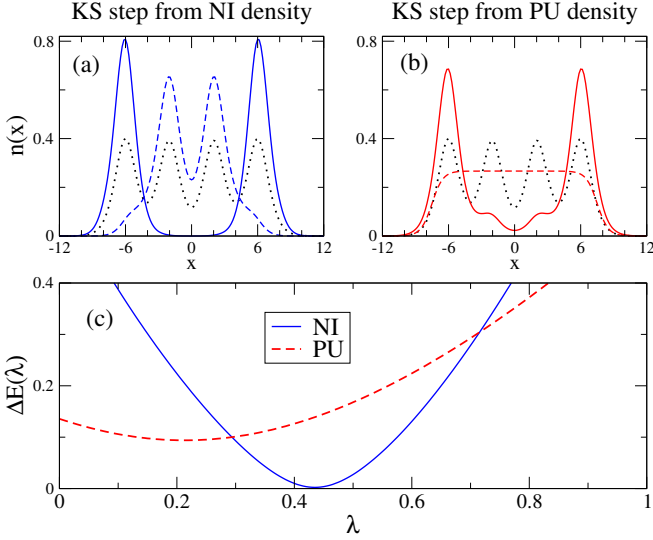Figure 6 models a weakly correlated system—a four

FIG. 7. A single step in the KS scheme for a strongly correlated system (H$_4$ with $R = 4$) away from two different initial densities: non-interacting electrons in the external potential (NI) and a pseudouniform electron density (PU). These initial densities are the dashed curves in (a) and (b), and the solid curves are the output densities for each KS step; for comparison the dotted curve is the exact density. The lower panel plots Eq. (22), the energy of the system as it interpolates from the input to the output density.

atom system with an interatomic spacing of $R = 2$—where a Slater determinant [70] of non-interacting electrons is a good approximation to the underlying wavefunction. But as we stretch the bonds to $R = 4$ for Fig. 7, strong static correlation arises, and the KS wavefunction is less like the true wavefunction of the interacting system than that of Fig. 6. Thus the density of a non-interacting system in the external potential is a poor start for the KS scheme, and energy differences from the ground-state are larger for the strongly correlated system

than for the weakly correlated system. Besides the scale, one might ask how the functional landscape differs between strongly correlated systems and weakly correlated systems. While the two NI curves in Figures 6 and 7 are deceptively similar, the PU curves begin to reveal the treacherous landscape of the strongly correlated system near the minimum.

We now look at the second iteration of the KS scheme to see if there is a difference between the strongly and weakly correlated systems. We choose the NI-path density from Fig. 7 with a good (but not optimal) mixing of $\lambda = 42\%$ as input into the KS equations. For the weakly correlated system of Fig. 6, the second KS step (not shown) looks much like the first step, though with a much smaller energy scale involved. Thus a fairly large λ may be used when correlations are weak, and convergence is rapid. But it is not the same for the strongly correlated system. As shown in Fig. 8, the next iteration of the KS procedure will not allow us to make the same giant stride as in the first iteration. For the new λ-mixed density, we again evaluate $\Delta E(\lambda)$ from Eq. (22) and find that it reaches a minimum much sooner. Thus a much smaller λ—around 6% as seen in the inset—must be chosen in order not to go far off track. Furthermore, choosing even the optimal λ does not result in a much better energy as it did in the first iteration. This makes convergence a long and difficult process, since we can only afford to take small steps.

In the last part of this section, we give some formulas which may aid in determining the optimal λ each step. We consider derivatives of $E_v(\lambda) \equiv E_v[n_\lambda]$ with respect to λ. For example, large $E_v''(\lambda) \equiv d^2E_v[n_\lambda]/d\lambda^2$ relative to the magnitude of $E_v'(\lambda) \equiv dE_v[n_\lambda]/d\lambda$ requires a smaller λ to lower the energy. Given some bound on $E_v''(\lambda)$, one could analytically determine a safe (i.e. not too large or too small) approximation to the optimal λ [71]. The derivatives of $E_v(\lambda)$ may be taken analytically [6, 72]:

$$E_v'(\lambda) = \int d^3r \left.\frac{\delta E_v[n]}{\delta n(\mathbf{r})}\right|_{n_\lambda(\mathbf{r})} \left(n_1(\mathbf{r}) - n_0(\mathbf{r})\right) = \int d^3r \left(v(\mathbf{r}) + v_{\text{HXC}}[n_\lambda](\mathbf{r}) - v_{\text{S}}[n_\lambda](\mathbf{r})\right)\left(n_1(\mathbf{r}) - n_0(\mathbf{r})\right) \quad (23)$$

$$E_v''(\lambda) = \int d^3r \int d^3r' \left(n_1(\mathbf{r}) - n_0(\mathbf{r})\right)\left(f_{\text{HXC}}[n_\lambda](\mathbf{r}, \mathbf{r}') - \chi_{\text{S}}^{-1}[n_\lambda](\mathbf{r}, \mathbf{r}')\right)\left(n_1(\mathbf{r}') - n_0(\mathbf{r}')\right), \quad (24)$$

where $n_1(\mathbf{r}) = n_{\text{out}}(\mathbf{r})$ and $n_0(\mathbf{r}) = n_{\text{in}}(\mathbf{r})$ for the current KS step of interest, the HXC kernel $f_{\text{HXC}}[n](\mathbf{r}, \mathbf{r}')$ is:

$$f_{\text{HXC}}[n](\mathbf{r}, \mathbf{r}') = \chi_{\text{S}}^{-1}[n](\mathbf{r}, \mathbf{r}') - \chi^{-1}[n](\mathbf{r}, \mathbf{r}'), \quad (25)$$

and $\chi_{\text{S}}^{-1}[n](\mathbf{r}, \mathbf{r}') = \delta v_{\text{S}}[n](\mathbf{r})/\delta n(\mathbf{r}')$ ($\chi^{-1}[n](\mathbf{r}, \mathbf{r}') = \delta v[n](\mathbf{r})/\delta n(\mathbf{r}')$) is the non-interacting (interacting) inverse density-density response matrix. Calculating $f_{\text{HXC}}[n](\mathbf{r}, \mathbf{r}')$ is quite challenging, and has recently been evaluated with time dependence for some simple systems [73].

We emphasize that $n_{\text{out}}(\mathbf{r})$ is a functional of $n_{\text{in}}(\mathbf{r})$ and does not depend on λ at all. Thus Eqs. (23) and (24) are strictly functionals of the input density $n_0(\mathbf{r})$ alone.

Towards the end of approximating the optimal λ, one may fit $E_v[n_\lambda]$ given some information on the derivatives.
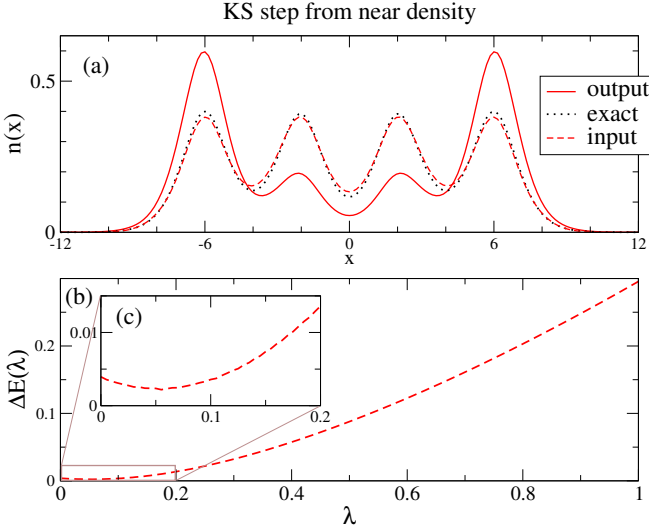
FIG. 8. Taking a second step in the KS scheme for a strongly correlated system (H_4 with $R = 4$). Panel (a) shows the input density which is near to the exact density (the $\lambda = 42\%$ density of the NI input density of Fig. 7) and the resulting output density, which is far from the ground-state. The lower panel (b) plots Eq. (22), and the inset (c) magnifies the small λ region.

At the end points the derivatives simplify to

$$E_v'(0) \equiv \int d^3r \left(v_{\mathrm{s},1}(\mathbf{r}) - v_{\mathrm{s},0}(\mathbf{r}) \right) \left(n_1(\mathbf{r}) - n_0(\mathbf{r}) \right) \quad (26)$$

$$E_v'(1) \equiv \int d^3r \left(v_{\mathrm{HXC}}^1(\mathbf{r}) - v_{\mathrm{HXC}}^0(\mathbf{r}) \right) \left(n_1(\mathbf{r}) - n_0(\mathbf{r}) \right), (27)$$

where $v_{\mathrm{s},j}(\mathbf{r}) = v_{\mathrm{s}}[n_j](\mathbf{r})$ and $v_{\mathrm{HXC}}^j(\mathbf{r}) = v_{\mathrm{HXC}}[n_j](\mathbf{r})$. We find that in many systems a Hermite spline fit [49] (using $E_v(0)$, $E_v(1)$, and the derivatives $E_v'(0)$ and $E_v'(1)$) is a good approximation to the energy curve $E_v(\lambda)$, or at least to where it attains the minimum. However, this fit requires an inversion to find $E_v(0)$ and $E_v'(0)$, which may be impractical for standard KS calculations.

C. Why convergence is difficult for strongly correlated systems

In this section, we discuss an important reason why convergence is difficult for strongly correlated systems, and mention some algorithms which counteract the underlying problem. Frequently, systems with strong static correlation possess a small gap [74], which in turn makes convergence difficult [58]. We can understand this difficulty by considering the non-interacting density-density response matrix $\chi_{\mathrm{s}}(\mathbf{r}, \mathbf{r}')$:

$$\chi_{\mathrm{s}}(\mathbf{r}, \mathbf{r}') = 2 \sum_{i \neq j}^{\infty} \frac{f_j - f_i}{\epsilon_j - \epsilon_i} \phi_i(\mathbf{r}) \phi_j^*(\mathbf{r}) \phi_i^*(\mathbf{r}') \phi_j(\mathbf{r}'), \quad (28)$$

where $0 \leq f_j \leq 1$ is the Fermi occupation of orbital $\phi_j(\mathbf{r})$. For a small gap system, $\epsilon_{\mathrm{LUMO}} - \epsilon_{\mathrm{HOMO}}$ is particu-
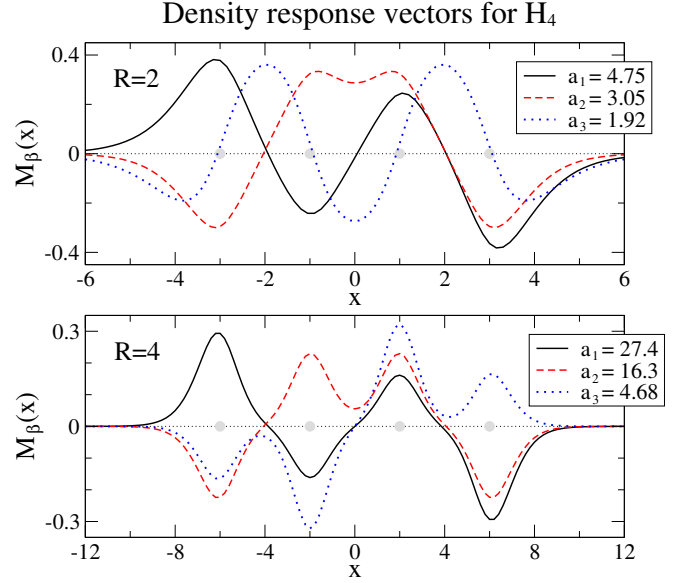

FIG. 9. The most important density response functions $M_\beta(x)$ from Eq. (29) and their response amplitudes a_β, for the weakly correlated system ($R = 2$) in the top panel, and the strongly correlated system ($R = 4$) in the bottom panel. The locations of the atoms are shown in solid grey circles.

larly small, making that term in $\chi_{\mathrm{s}}(\mathbf{r}, \mathbf{r}')$ especially large. This means that small changes in the KS potential can produce large changes in the density, which makes convergence in the KS scheme difficult. We can visualize this property by performing a singular value decomposition on $\chi_{\mathrm{s}}(\mathbf{r}, \mathbf{r}')$, as in Eq. (16). Equivalently, since $\chi_{\mathrm{s}}(\mathbf{r}, \mathbf{r}')$ is symmetric in $\mathbf{r}, \mathbf{r}'$, we can diagonalize $-\chi_{\mathrm{s}}(\mathbf{r}, \mathbf{r}')$:

$$\chi_{\mathrm{s}}(\mathbf{r}, \mathbf{r}') = -\sum_{\beta=1}^{\infty} a_\beta M_\beta(\mathbf{r}) M_\beta(\mathbf{r}'), \quad (29)$$

where $M_\beta(\mathbf{r})$ (a_β) are the eigenvectors (eigenvalues) of $-\chi_{\mathrm{s}}(\mathbf{r}, \mathbf{r}')$. Since $\chi_{\mathrm{s}}(\mathbf{r}, \mathbf{r}')$ is negative definite, we can order $a_\beta \geq a_{\beta+1} > 0$. The breakdown in Eq. (29) physically means that a change in the KS potential along the direction $-M_\beta(\mathbf{r})$ produces a change in the density along $M_\beta(\mathbf{r})$ with a magnitude given by a_β, at least to first order. We therefore call $M_\beta(\mathbf{r})$ the density response vectors and a_β the response amplitudes of $\chi_{\mathrm{s}}(\mathbf{r}, \mathbf{r}')$. The amplitudes depend on the normalization of $M_\beta(\mathbf{r})$, and the standard squared (L^2) norm is not the most natural choice. Because $M_\beta(\mathbf{r})$ corresponds to a change in density, we choose $\int d^3r |M_\beta(\mathbf{r})| = 2$ so that $M_\beta(\mathbf{r})$ can be thought of as moving an electron from one region (where $M_\beta(\mathbf{r}) < 0$) to another (where $M_\beta(\mathbf{r}) > 0$). Finally, because a_β are ordered by importance, $\chi_{\mathrm{s}}(\mathbf{r}, \mathbf{r}')$ can be accurately and efficiently represented by truncating the sum once a_β drops below some tolerance.

We can easily find the density response vectors $M_\beta(x)$ for the 1d H_4 systems we have already discussed at length, which allows us to diagnose our convergence difficulties. In Fig. 9, we plot the first few most important

$M_\beta(x)$. The first two $(\beta = 1, 2)$ look similar for the weakly correlated and the strongly correlated systems, though the response amplitudes a_β are quite different. If the potential changes in the direction $-M_1(x)$, it drives a strong density response in the direction $M_1(x)$ due to the large response amplitude $a_1 = 4.75$ at $R = 2$ and $a_2 = 27.4$ at $R = 4$. Luckily, we can assume reflection symmetry, so that in the iteration of the KS equations we do not have to worry about contributions from these $\beta = 1$ terms. But now consider the symmetric $\beta = 2$ terms. If the KS potential changes in the direction $-M_2(x)$, the density will respond by changing in the direction $M_2(x)$, and the response amplitude is very strong for the $R = 4$ system $(a_2 = 16.3)$.

These (ground-state) response properties can be used to explain the problems that we have converging the strongly correlated H_4. If the initial KS potential puts most of the density around the central two atoms, to compensate the next trial KS potential (10) will increase in the central region and decrease for the edge atoms. In response, the new density will place too many electrons on the edge atoms. We have already seen this in Figures 6 and 7 with the NI starting densities. The reverse can also happen, where most of the input density is on the edge atoms, and the output density is more centralized. For the strongly correlated H_4, this "sloshing" back and forth can be particularly strong because the response amplitude a_2 is quite large – this problem plagues densities even very close to the ground state, as seen in Fig. 8. As $R \to \infty$, a_2 diverges, making it more and more difficult to converge. To ameliorate these problems, some convergence schemes artificially increase the gap [57] or populate otherwise unoccupied orbitals [75]. For other discussions on this matter, see Ref. [76] and for implications for time-dependent DFT, Ref. [77].

D. Convergence as correlations grow stronger

In this section we explore convergence within the simplest density functional approximation, the local density approximation (LDA) [4], in order to understand some basic limits on convergence as well as its dependence on the KS gap, i.e. the HOMO-LUMO gap. A simple expression for the LDA is available for our model 1d systems [28, 52]. We expect the LDA to converge in a similar way to the exact functional, especially when the KS gap of the system is close for both self-consistent LDA and exact solutions [78]. We therefore use it to study more broadly the convergence behavior of the KS scheme applied to H_2 with variable bond length. As before, changing the bond length allows us to tune the strength of the correlation: at small bond lengths the system is weakly correlated and at large bond lengths strong static correlation arises [28]. To aggravate convergence difficulties, we choose the initial density to be entirely centered on one atom [6], and determine the λ values for which the KS scheme will converge, as well as how quickly. Furthermore, we en-
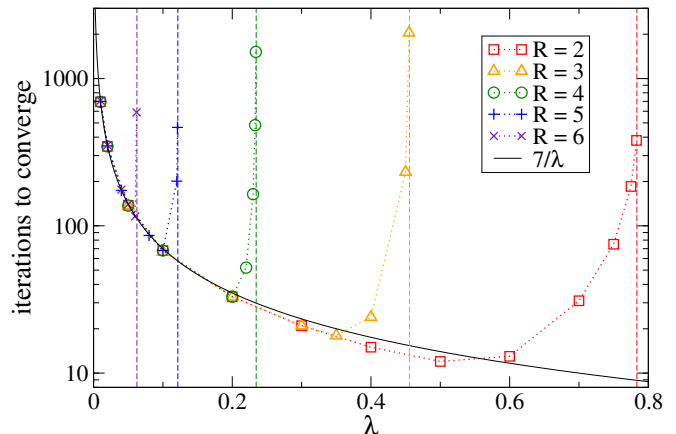

FIG. 10. The number of iterations required to converge an LDA calculation to $\eta < 10^{-8}$ (12), as a function of λ, for various bond-lengths R of the H_2 molecule, starting with an initial density of H^- on the left atom. The asymptotic form for small λ can be well-approximated by $7/\lambda$ for the data shown.

force spin-symmetry, so while the restricted LDA energy is wrong in the $R \to \infty$ limit [28], we expect to see convergence behavior similar to the exact functional [6].

In Fig. 10, we plot the number of iterations required to converge an LDA calculation to $\eta < 10^{-8}$ as a function of λ, for a variety of bond lengths R. Each curve ends at $\lambda_c(R)$, the largest λ for which the damped KS algorithm converges from this initial density. For a weakly correlated system (e.g. $R = 2$), a very large λ will produce convergence, and the optimal λ to converge in the fewest iterations is also fairly large (around 0.5 for $R = 2$). As the bond length is stretched, both the critical λ, $\lambda_c(R)$, as well as the optimal $\lambda_O(R)$ decrease. In response, the minimum number of iterations $N_{\min}(R)$ to converge to a tolerance $\eta < 10^{-8}$, increases. For example, $N_{\min}(R = 2) = 12$ for $\lambda_O(R = 2) \approx 0.5$. Considering the iterations it takes to converge as a function of λ, we see that as λ decreases past the optimal λ, it begins to take longer to converge the calculation. For $\lambda \to 0$, we approach an asymptote that appears valid for all values of R, given this initial starting point in the H_2 system: $N_{\text{asym}}(\lambda) = 7/\lambda$. While this is by no means a universal asymptote for all systems, we recognize there is a fundamental limit to how quickly we can converge as $\lambda \to 0$.

In Fig. 11, we plot the convergence-critical λ value as a function of the bond length R, as well as the KS gap of both the LDA and exact systems. The LDA KS gap decays at about the same rate as the critical λ, an observation that makes sense given that the KS gap has such an important role in convergence – the smaller the gap the more difficult it is to converge the calculation [78]. For bond lengths $R \lesssim 4$, the LDA KS gap is quite close to the exact KS gap, so that we expect similar convergence behavior for the exact functional. However, as R increases the true KS gap decays more quickly than the
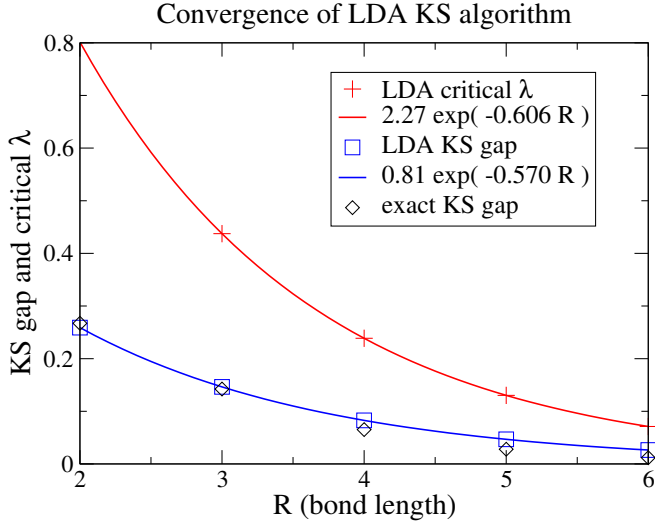
FIG. 11. Plotting λ_c for an LDA calculation, as a function of the bond length R of a stretched hydrogen molecule, starting with the exact H^- density on one atom as well as KS gaps for both the LDA and exact systems.

LDA KS gap, so that the exact calculation has an even greater difficulty converging [6]. It could be that some values of λ larger than λ_c allow for convergence if the density fortuitously lands close enough to the ground state in some iteration, but there is no systematic approach to find these λ.

E. Classifying convergeability

In this section, we want to mathematically investigate the the space of densities that allow convergence and how quickly that occurs. That is, given some initial density and a fixed value of λ, can we determine whether the KS scheme will converge within some given number of iterations? With λ too large, the KS scheme will be doomed to repeatedly overstep the ground-state density.

To quantify these ideas, define $\eta^M[n](\lambda)$ to be the value of η defined by Eq. (12) after M iterations of the KS equations with a fixed mixing of λ, starting with the input density $n(\mathbf{r})$. Then define the density set:

$$S_\zeta^M(\lambda) \equiv \big\{ n(\mathbf{r}) \text{ s.t. } \eta^M[n](\lambda) < \zeta \big\}. \qquad (30)$$

This set describes the densities $n(\mathbf{r})$ which converge to $\eta < \zeta$ in a finite number of iterations (M), given a fixed-λ iteration of the KS equations. For example, $S_\zeta^1 \equiv S_\zeta^1(\lambda = 1)$ is the set of input densities $n_{\text{in}}(\mathbf{r})$ that are within $\eta < \zeta$ of their output densities. (For one step, λ does not matter.) This set (30) allows us to quantify the different levels of convergence hell. S_ζ^1 is the lowest level, and includes the ground-state density. $S_\zeta^2(1)$ is the second level, and also includes the ground-state density. As M becomes large (but remains finite), $S_\zeta^M(1)$ reaches out to the Mth level of hell: the set of densities which converge
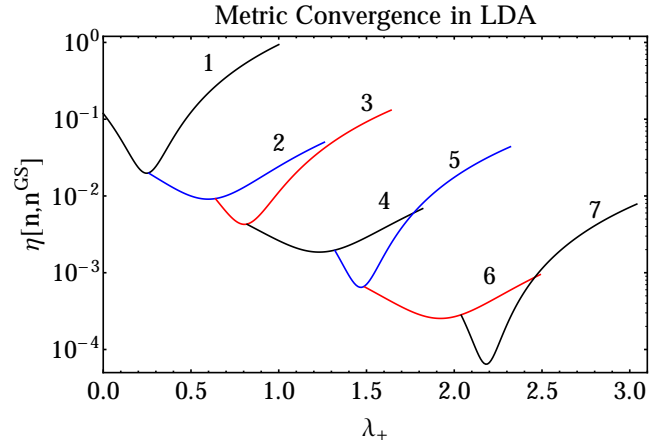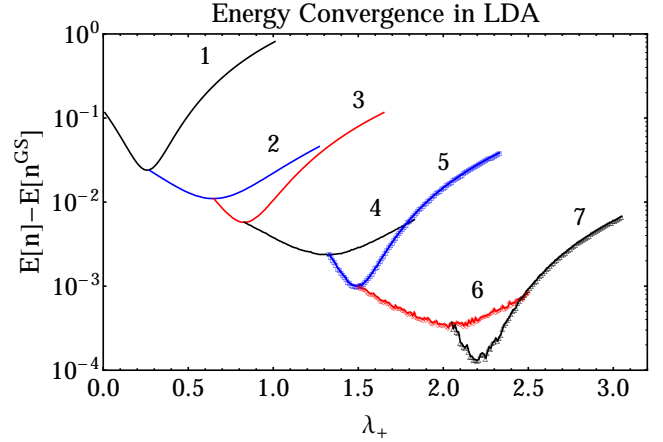

FIG. 12. The first few steps (numbered) in the KS scheme from some arbitrary starting density for H_4 with $R = 4$ in the LDA approximation. Numerical precision makes the energy data noisy. Metric distances are compared with the LDA ground state. Figure (a) plots the energy and (b) the metric as a function of the accumulated λ step. The density $n_\lambda(x)$ with the lowest metric distance is not the energetic minimum, but they are fairly close.

to within $\eta < \zeta$ within a finite number of full-KS-step iterations. All other densities belong to the $\lambda = 1$ limbo density set, densities which are doomed to wander for (essentially) all eternity, never to converge. Similarly, there are less-strict convergence sets for $\lambda < 1$, which describe a sort of density purgatory.

It might be hoped to connect these abstract convergence sets with some concrete measure, say some metric between the ground-state density and the density inputted into the KS scheme, $\eta[n, n^{\text{gs}}]$. Here we simply define the metric similarly to our η convergence quanti-

fier:

$$\eta[n_1, n_2] = \int d^3r \left(n_1(\mathbf{r}) - n_2(\mathbf{r}) \right)^2 / N^2. \quad (31)$$

The idea of a metric on the set of densities is not new [79, 80]. Unfortunately, current metrics are not guaranteed to correlate e.g. a given input density $n(\mathbf{r})$ with a given convergence set $S_\zeta^M(\lambda)$. That is, there is likely no function $g_\zeta^M(\lambda)$ for which $\eta[n, n^{\mathrm{gs}}] < g_\zeta^M(\lambda) \implies n(\mathbf{r}) \in S_\zeta^M(\lambda)$. In Fig. 12 we show why. For λ_+ the accumulated λ throughout the KS scheme, we see that the metric $\eta[n_{\lambda_+}, n^{\mathrm{gs}}]$ tracks well with the how close the energy $E_v[n_{\lambda_+}]$ is to the ground state energy (at least for this example, 1d H_4 in LDA). Despite this nice relationship between the energy and the metric, a small $\eta[n, n^{\mathrm{gs}}]$ does not necessarily mean we can take a large step in λ each iteration. Therefore we do not know how many steps it will take nor how small a λ is required based on the metric alone. More physically motivated metrics might remedy this issue, but we must leave this question open.

F. Spin DFT

In this section we extend the exact functional to include spin dependence. We test the exact spin-dependent functional on the case of stretched H_2, starting our KS scheme with a broken-spin-symmetry solution, to determine whether or not the exact functional will find the correct spin-singlet ground state [6].

Treating the up-spin and down-spin electrons separately leads to much improved density functional approximations, as well as new challenges [81, 82]. If an unbalanced spin-state is provided as input to the KS scheme, approximate spin-density functionals may find a broken break spin symmetry when the ground state should be a singlet. This is the case for many open-shell systems as bonds are stretched. The simplest such system, and a paradigm of DFT failures, is stretched H_2 [28, 83–85]. In this case, it is clear that the exact XC spin-density functional does not break symmetry at the solution density, since the ground state of any two-electron system is a singlet (in the absence of external magnetic fields [84]). This is true of both the interacting wavefunction and the KS Slater determinant, which is then just a doubly occupied molecular orbital.

To investigate these issues, we must first add spin-dependence to our functional, which is simple enough in principle. The added challenge is needing the ability to solve an interacting system with different potentials for spin-up and spin-down electrons, i.e. electrons in a collinear magnetic field. Similar to (18), the HXC potential for spin-σ electrons is:

$$v_{\mathrm{HXC},\sigma}[n_\uparrow, n_\downarrow](\mathbf{r}) = v_{\mathrm{s}}[2n_\sigma](\mathbf{r}) - v_\sigma[n_\uparrow, n_\downarrow](\mathbf{r}), \quad (32)$$

where the KS potential for the up electrons can be inverted independently of the down electrons by doubly
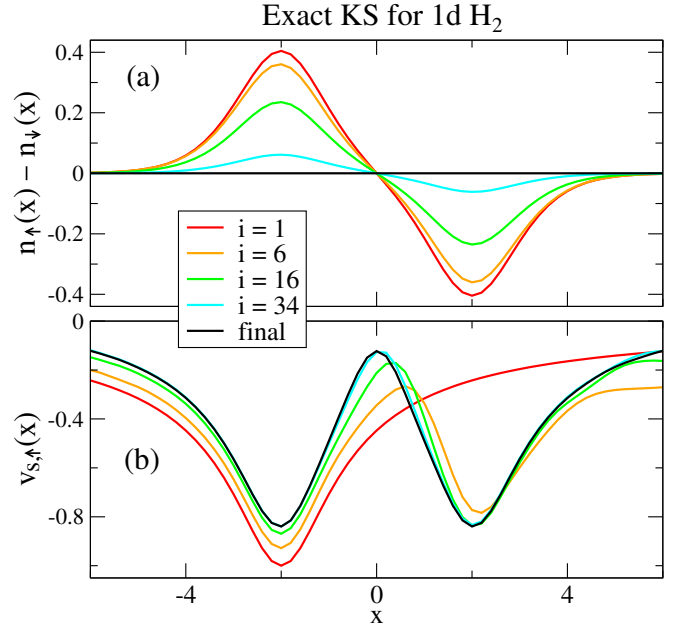

FIG. 13. Starting an exact KS calculation of stretched H_2 with a spin-polarized density still converges to the correct spin-singlet density. Through the iterations i, we plot (a) the polarization density $n_\uparrow(x) - n_\downarrow(x)$ and (b) the up KS potentials $v_{\mathrm{s},\uparrow}(x)$; the down potentials are the mirror images.

occupying the up density [86] (and vice versa for down electrons), and $v_\sigma[n_\uparrow, n_\downarrow](\mathbf{r})$ is the spin-σ potential necessary to produce spin densities $n_\uparrow(\mathbf{r})$ and $n_\downarrow(\mathbf{r})$ from an interacting Hamiltonian. We now investigate the use of the exact spin-dependent functional in a system where standard approximate functionals have multiple stationary points.

To test whether the exact functional can find the singlet solution for the stretched H_2 case, we start the exact KS calculation with a spin-polarized initial density, with the up electron on the left atom and the down electron on the right. With this input, the KS scheme using the local spin-density approximation converges to a broken symmetry solution [28]. But as seen in Fig. 13, the exact functional finds the correct spin-singlet density without much trouble. (For this system, a large density mixing was used, namely $\lambda = 50\%$.) So long as the spin-densities are v-representable, the arguments of Ref. [63] apply, and there is only one stationary point of the exact functional – the true ground-state density. This is true not only in 1d (as we have illustrated) but also in 3d.

G. Non v-representable densities

An important question that has haunted density functional theory since the proofs of Hohenberg and Kohn is that of v-representability [47], i.e., for a given density $n(\mathbf{r})$, does there exist a one-body potential $v[n](\mathbf{r})$ for which it is the ground-state density? The constrained-

search formulation of Levy [12] and of Lieb [7] bypasses this issue by defining the functional $F[n]$ as an infimum over a given class of wavefunctions. But our methodology of performing both interacting and non-interacting inversions essentially requires v-representability in both the interacting and non-interacting systems. (In fact, $v_{\text{HXC}}[n](\mathbf{r})$ is ill-defined if $n(\mathbf{r})$ is not v-representable [7, 41].) In all our calculations to date, we have had no difficulty with v-representability, but in the present section, we use explore its meaning in more detail.

To be clear, we consider a density v-representable if it is *ensemble* v-representable. The generalization to mixed states (ensembles) is important for degenerate systems, where not every density comes from a pure-state wavefunction [7, 39, 56]; these practical details impact the calculations for and the values of the functionals $F[n]$ and $T_{\text{s}}[n]$ [6, 7, 87], but they are not our primary concern. In addition, we focus on *non-interacting* v-representability; the challenges for interacting v-representability are similar, though the sets of interacting and non-interacting v-representable densities may in principle be different.

Definitive work by Chayes *et al.* [88] proves that on a grid, certain simple restrictions on the density determine the set of ensemble v-representable densities (in both interacting and non-interacting cases). This result explains why we were always able to find potentials for a given density on a grid in 1d, where there is no degeneracy except for spin. The work of Chayes *et al.* is reassuring, but not the final word on v-representability. On a grid, the kinetic energy operator (proportional to the Laplacian) is always bounded, whereas in the continuum it is not. In such cases, inverting a density for the KS potential as in Eq. (13) may lead to unacceptable divergences, even for reasonable densities. Proofs of v-representability on a grid [54] therefore do not guarantee v-representability in the continuum. Complicating matters, properties which make for reasonable densities and potentials differ based on the dimensionality of the problem [7]. In this section, we therefore move away from our 1d grids and instead concentrate on real 3d systems in the continuum.

In principle, one can invert any density $n(\mathbf{r})$ with $N \leq 2$ for its KS potential $v_{\text{s}}[n](\mathbf{r})$, as in Eq. (13). Such an inversion, however, may lead to a potential which is singular and which does not have a well-defined ground state. In order to avoid these problems, the potential should satisfy two key properties: (1) the KS Hamiltonian (5) being bounded from below, and (2) the KS Hamiltonian being self adjoint. Properties which make the potential reasonable translate into properties that the density should satisfy. In three dimensions, our reasonable potentials are in the set $L^{3/2} + L^\infty$, whose dual is $L^1 \cap L^3$, a good start for the set of reasonable densities [7]. The L^p space consists of functions whose p norm is finite:

$$L^p \equiv \left\{ f(\mathbf{r}) \ : \ \left(\int d^3r\, f^p(\mathbf{r}) \right)^{1/p} < \infty \right\}. \quad (33)$$

Thus our densities $n(\mathbf{r})$ should at least be in $L^1 \cap L^3$,

and our potentials in $L^{3/2} + L^\infty$. (This set includes Coulomb potentials [7].) For a density whose inverted potential is *not* in $L^{3/2} + L^\infty$ we say this density is non-v-representable.

To avoid unphysical densities, one should impose non-negativity and finite kinetic energy on the density, as articulated first by Lieb [7, 41, 88]:

$$\int d^3r\, n(\mathbf{r}) = N < \infty, \quad n(\mathbf{r}) \geq 0 \ \ \forall\ \mathbf{r}, \quad T_{\text{s}}^{\text{vW}}[n] < \infty, \quad (34)$$

where

$$T_{\text{s}}^{\text{vW}}[n] \equiv \int d^3r\, \frac{|\nabla n(\mathbf{r})|^2}{8\, n(\mathbf{r})}. \quad (35)$$

We refer to such Lieb-allowed densities (which satisfy Eq. (34)) as reasonable. Reasonable densities comprise a subset of $L^1 \cap L^3$ (by Sobolev's inequality [7]), so they have many useful properties. For example, for a reasonable density $n(\mathbf{r})$, $|V[n]| < \infty$ if the potential $v(\mathbf{r})$ is also reasonable (i.e. in $L^\infty + L^{3/2}$). A density $n(\mathbf{r})$ which fails to satisfy Eq. (34) can safely be regarded as having an infinite $F[n]$ (or $T_{\text{s}}[n]$ for non-interacting systems) [7], and thus will be avoided in any iteration of the Kohn–Sham equations. On the other hand, there always exists a v-representable density $\tilde{n}(\mathbf{r})$ that approximates a reasonable density $n(\mathbf{r})$ to any desired accuracy, for which the energies $F[\tilde{n}]$ and $T_{\text{s}}[\tilde{n}]$ may be calculated [7, 41]. In the remainder of this section, we will explore such an example within the realm of non-interacting v-representability, or v_{s}-representability for short.

We consider a density which satisfies Eq. (34) but which is not v_{s}-representable. Inspired by the fourth example of Englisch and Englisch [38], we choose:

$$n_{\text{P}}(\mathbf{r}) = A\big(1 + |r-1|^{3/4}\big)^2 e^{-2r}, \quad (36)$$

where we normalize to two electrons with

$$A = \frac{256 e^2}{\pi\,(596 e^2 + 273\,B + 506\,C)} \quad (37)$$

$$\approx 0.196521 \quad (38)$$

with

$$B = \sqrt{2\pi}\left(1 + \frac{2}{\sqrt{\pi}} \int_0^{\sqrt{2}} dt \exp(t^2)\right) \quad (39)$$

$$C = \frac{3}{2^{\frac{3}{4}}}\left(\Gamma\left[\frac{3}{4}\right] - \int_0^2 dt\, \frac{\exp(t)}{t^{\frac{1}{4}}}\right). \quad (40)$$

This pathological density $n_{\text{P}}(\mathbf{r})$ is not v_{s}-representable due to the kink encountered at $r = 1$, which would require an inadmissible infinite-discontinuity in the KS potential. To see this, we attempt to invert $n_{\text{P}}(\mathbf{r})$ for its KS potential via Eq. (13):

$$v_{\text{s}}[n_{\text{P}}](\mathbf{r}) \overset{?}{=} \frac{1}{2} - \frac{1}{r} + \frac{3}{4\left(1 + |r-1|^{3/4}\right)}\left[-\frac{1}{8|r-1|^{5/4}}\right.$$
$$\left. + \frac{\delta(r-1)}{|r-1|^{1/4}} - \frac{\text{sgn}(r-1)}{|r-1|^{1/4}}\left(1 - \frac{1}{r}\right)\right], \quad (41)$$
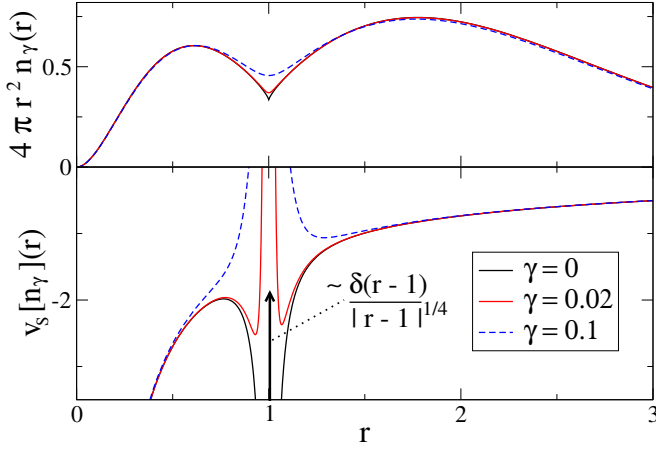
FIG. 14. Inverting $n_\gamma(r)$ of Eq. (49) for the KS potential. As γ becomes smaller and smaller, the changes in potential near $r = 1$ become larger and larger.

where we have used $\partial_x |x| = \text{sgn}(x)$, $\partial_x^2 |x| = 2\delta(x)$, and $\text{sgn}(x)$ is the sign function. The worst offender is the term proportional to $\delta(r-1)/|r-1|^{1/4}$ which fails to be in the set $L^{3/2} + L^\infty$. This makes $n_\text{P}(\mathbf{r})$ non-v_s-representable, since it may not even be the ground state of Eq. (41). Furthermore, calculating $T_\text{s}[n]$ using the second-derivative formula of Eq. (8) is ill-defined, due to this discontinuity. Nevertheless, $n_\text{P}(\mathbf{r})$ is reasonable: its $T_\text{s}^\text{vW}[n_\text{P}]$ is finite, as we will soon show. So, despite the density being reasonable, it is non-v_s-representable.

We obtain $T_\text{s}^\text{vW}[n_\text{P}]$ by first calculating its kinetic energy density. Due to spherical symmetry, we have:

$$t_\text{s}^\text{vW}[n_\text{P}](r) = \frac{1}{2}\left(\frac{d}{dr}\sqrt{n_\text{P}(r)}\right)^2 \tag{42}$$

$$= \frac{A}{2}\left(-1 - |r-1|^{3/4} + \frac{3\,\text{sgn}(r-1)}{4\,|r-1|^{1/4}}\right)^2 e^{-2r}, \tag{43}$$

so that

$$T_\text{s}^\text{vW}[n_\text{P}] = 4\pi \int_0^\infty dr\, r^2\, t_\text{s}^\text{vW}[n_\text{P}](r) \tag{44}$$

$$= \frac{A\pi}{128e^2}\left(40e^2 + 93\,B - 13\,C\right) \tag{45}$$

$$\approx 0.996519. \tag{46}$$

Calculating $T_\text{s}[n_\text{P}]$ via the second-derivative formula (8) seems like a simple integration by parts:

$$\left.\begin{aligned} T_\text{s}[n] &= -\frac{1}{2}\int d^3r\,\sqrt{n(\mathbf{r})}\nabla^2\sqrt{n(\mathbf{r})} \\ &= -\int d^3r\, n(\mathbf{r})\, v_\text{s}[n](\mathbf{r}) \end{aligned}\right\} \quad (N \leq 2), \tag{47}$$

but due to the discontinuities in $v_\text{s}[n_\text{P}](\mathbf{r})$ (41), this integral is ill-defined for $n_\text{P}(\mathbf{r})$.

We now illustrate how to obtain a v_s-representable density that is arbitrarily close to our reasonable density $n_\text{P}(\mathbf{r})$. As a bonus, this procedure will also give a
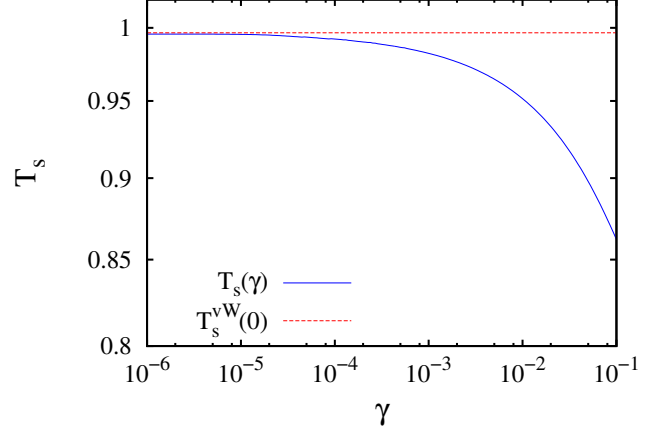

FIG. 15. Kinetic energy convergence of $n_\text{P}(r)$ from Eq. (49) by smoothing out the kink as in Eq. (36). While the von Weizsäcker kinetic energy (vW) may be evaluated and integrated using only one derivative of the density, higher order derivatives of the density develop nonintegrable features.

well-defined kinetic energy using the second-derivative formula. Consider a function $f_\gamma(x)$ that smooths out the $|r-1|$ in Eq. (36), but which has a parameter which can be continuously adjusted so that $\lim_{\gamma\to 0} f_\gamma(r-1) = |r-1|$. We choose

$$f_\gamma(x) = \sqrt{x^2 + \gamma^2}, \tag{48}$$

setting

$$n_\gamma(\mathbf{r}) = A_\gamma\left(1 + f_\gamma^{3/4}(r-1)\right)^2 e^{-2r}. \tag{49}$$

(Note that the density must be renormalized for each value of γ.) For small γ, the metric distance between $n_\text{P}(\mathbf{r})$ and $n_\gamma(\mathbf{r})$, $\eta[n_\text{P}, n_\gamma]$ (31), is proportional to $\gamma^{2.5}$; and $n_\gamma(\mathbf{r})$ remains v-representable for all $\gamma > 0$. In the iterations of the Kohn–Sham scheme, tolerances between densities are already built into the method—namely as in Eq. (12)—so we need no greater accuracy than that when finding a v-representable density close enough to the target density.

As already mentioned, even though $T_\text{s}^\text{vW}[n_\text{P}]$ is finite, $T_\text{s}[n_\text{P}]$ via Eq. (47) is ill-defined. But by using the smoothed density of Eq. (49), we can calculate $T_\text{s}[n_\gamma]$ and take the limit $\gamma \to 0$ (see Fig. 15). The result is the the same as $T_\text{s}^\text{vW}[n_\text{P}]$, and this must be so based on simple mathematical considerations [88]. Two conjectures might be made after consider the foregoing:

1. A density being v-representable requires some bounds on the Laplacian (or second derivative) of the density. On a grid, this is not an issue because the Laplacian is always bounded.

2. Finite energies $F[n]$ and $T_\text{s}[n]$ may be extracted from reasonable but non-v-representable densities.

This can be done by suitably smoothing (or discretizing) the density and carefully taking limits, so as to remove divergent terms. For $N \leq 2$, $T_s^{vW}[n]$ should give the limit of $T_s[n]$ properly, and for $N > 2$ one should be able to use

$$T_s[n] = \sum_{j=1}^{N/2} \int d^3r \, |\nabla \phi_j(\mathbf{r})|^2, \tag{50}$$

to avoid any singular divergences from second derivatives.

It is important to note that all of our numerical inversions have used pure-state wavefunctions. This is justified for spin-singlet 1d systems and for this simple spin-singlet example in 3d. In systems with degeneracy, however, the ensemble formulation of DFT should be used, not only because the ensemble $E_v[n]$ is convex [6], but also because the class of pure-state v-representable densities is smaller than the class of ensemble v-representable densities [7, 41]. Outside of this section, we always worked on a grid, which means that v-representability difficulties were not an issue [88]. We found no cases where, as the grid spacing goes to zero, the potential diverged as in the example here.

V. CONCLUSIONS

Our investigations into the exact functional demonstrate that it is possible to solve the Kohn–Sham equations with the exact XC functional for simple model systems sometimes at great computational cost. Our calculations involve mapping the functional landscape for more than just the ground-state density, enabling us to address questions of convergence within the KS scheme. We tested many systems, and found that strongly correlated systems pose a greater challenge, not only from a theoretical standpoint in finding accurate approximations, but also practically within the KS scheme, where smaller steps must be taken (or more sophisticated methods used) to converge the calculation. In a word, the exact functional landscape for strongly correlated systems is more treacherous, but not impossible, for a simple KS algorithm to navigate.

Despite the surmountable convergence difficulties for strongly correlated systems, the only stationary point of the KS equations is the ground-state density of the original problem, given v-representable densities as inputs. This is simply a reaffirmation of the HK theorem, that there is a one-to-one correspondence between ground state densities and potentials. This is the case even for stretched systems, where approximate functionals would prefer to break spin symmetry; the exact spin-density functional has only one stationary point, at the correct ground-state spin densities. All changes in density away from that point cause the energy to rise. Thus the lowest energy stationary point with an approximate functional

has the same energy landscape as the true functional, and should be treated as the prediction for the energy with that approximation, regardless of how many symmetries have been broken. This reaffirms the conclusions of Ref. [84].

The density mixing algorithm used to prove convergence of the KS scheme is one of the simplest ways to explore the infinite-dimensional set of possible densities, and it provides insight into the gradient-descent nature of the KS scheme. While this algorithm is too primitive for modern practical implementations, its main purpose here is to provide a definite framework in which convergence questions can be studied.

There is another avenue of research, but which cannot be pursued in these model 1d systems: the effects of orbital degeneracy within exact KS theory, especially due to angular momentum. An ensemble of degenerate densities may easily not be pure-state v-representable [7, 41], and the extent of the challenges for exact DFT warrants investigation. Unfortunately, this avenue cannot be explored for these 1d systems, in which there is no angular momentum.

Finally, we discuss the consequences of our example of a non v-representable density. The example we give is a reasonable density, meaning it is in the domain on with the Levy-Lieb density functional is defined: it is normalized, non-negative, and has finite kinetic energy. Consistent with the proof of Chayes et. al. [88], on any finite grid, it has a well-behaved Kohn-Sham potential. But as the grid-spacing is brought to zero, divergences appear in that potential, so that it is ill-defined in the continuum limit. So this is an example of a density that is v-representable on a lattice, but is not v-representable in the continuum. Similarly, one can remain in the continuum and introduce a small parameter (γ) which rounds off the cusp in the density. For any finite value of γ, no matter how small, the potential is finite and well-behaved. Thus our cuspy density is arbitrarily close to a v-representable density. These are the standard arguments given in the physics literature for why v-representability is not an issue in DFT.

But our example shows that there is still something to worry about. Either regularization procedure (finite grid spacing or finite γ) fails in the limit, and anyone doing an inversion on such a density should check their KS potential converges to a well-defined limit. Our example density fails this test.

The important question is not whether some artificially created density is v-representable or not. The real question is, given the densities of atoms, molecules, and solids, i.e., densities generated by solving the Schrödinger equation with Coulomb interactions, are there features like that of our example that produce ill-behaved KS potentials? This is all that matters, and practical experience suggests that such situations are rare, if they occur at all.

[1] L. H. Thomas, "The calculation of atomic fields," Math. Proc. Camb. Phil. Soc. **23**, 542–548 (1927).

[2] E. Fermi, "Eine statistische Methode zur Bestimmung einiger Eigenschaften des Atoms und ihre Anwendung auf die Theorie des periodischen Systems der Elemente (a statistical method for the determination of some atomic properties and the application of this method to the theory of the periodic system of elements)," Zeitschrift für Physik A Hadrons and Nuclei **48**, 73–79 (1928).

[3] E. Schrödinger, "An undulatory theory of the mechanics of atoms and molecules," Phys. Rev. **28**, 1049–1070 (1926).

[4] W. Kohn and L. J. Sham, "Self-consistent equations including exchange and correlation effects," Phys. Rev. **140**, A1133–A1138 (1965).

[5] P. Hohenberg and W. Kohn, "Inhomogeneous electron gas," Phys. Rev. **136**, B864–B871 (1964).

[6] Lucas O. Wagner, E. M. Stoudenmire, Kieron Burke, and Steven R. White, "Guaranteed convergence of the kohn-sham equations," Phys. Rev. Lett. **111**, 093003 (2013).

[7] Elliott H. Lieb, "Density functionals for coulomb systems," Int. J. Quantum Chem. **24**, 243–277 (1983).

[8] John P. Perdew and Yue Wang, "Accurate and simple analytic representation of the electron-gas correlation energy," Phys. Rev. B **45**, 13244–13249 (1992).

[9] Axel D. Becke, "Density-functional thermochemistry. iii. the role of exact exchange," J. Chem. Phys. **98**, 5648–5652 (1993).

[10] John P. Perdew, Kieron Burke, and Matthias Ernzerhof, "Generalized gradient approximation made simple," Phys. Rev. Lett. **77**, 3865–3868 (1996), *ibid.* **78**, 1396(E) (1997).

[11] K. Burke, "Perspective on density functional theory," J. Chem. Phys. **136** (2012).

[12] Mel Levy, "Universal variational functionals of electron densities, first-order density matrices, and natural spin-orbitals and solution of the v-representability problem," Proceedings of the National Academy of Sciences of the United States of America **76**, 6062–6065 (1979).

[13] J. P. Coe, K. Capelle, and I. D'Amico, "Reverse engineering in many-body quantum physics: Correspondence between many-body systems and effective single-particle equations," Phys. Rev. A **79**, 032504 (2009).

[14] M. Levy and J.P. Perdew, "Hellmann-feynman, virial, and scaling requisites for the exact universal density functionals. shape of the correlation potential and diamagnetic susceptibility for atoms," Phys. Rev. A **32**, 2010 (1985).

[15] John P. Perdew and Stefan Kurth, "Density functionals for non-relativistic Coulomb systems in the new century," in *A Primer in Density Functional Theory*, edited by Carlos Fiolhais, Fernando Nogueira, and Miguel A. L. Marques (Springer, Berlin / Heidelberg, 2003) pp. 1–55.

[16] John P. Perdew, Adrienn Ruzsinszky, Jianmin Tao, Viktor N. Staroverov, Gustavo E. Scuseria, and Gabor I. Csonka, "Prescription for the design and selection of density functional approximations: More constraint satisfaction with fewer fits," The Journal of Chemical Physics **123**, 062201 (2005).

[17] John P. Perdew and Mel Levy, "Physical content of the exact kohn-sham orbital energies: Band gaps and derivative discontinuities," Phys. Rev. Lett. **51**, 1884–1887 (1983).

[18] L. J. Sham and M. Schlüter, "Density-functional theory of the energy gap," Phys. Rev. Lett. **51**, 1888–1891 (1983).

[19] C. O. Almbladh and A. C. Pedroza, "Density-functional exchange-correlation potentials and orbital eigenvalues for light atoms," Phys. Rev. A **29**, 2322–2330 (1984).

[20] C. J. Umrigar and Xavier Gonze, "Accurate exchange-correlation potentials and total-energy components for the helium isoelectronic series," Phys. Rev. A **50**, 3827–3837 (1994).

[21] R. van Leeuwen and E. J. Baerends, "Exchange-correlation potential with correct asymptotic behavior," Phys. Rev. A **49**, 2421–2431 (1994).

[22] C. Filippi, C. J. Umrigar, and M. Taut, "Comparison of exact and approximate density functionals for an exactly soluble model," The Journal of Chemical Physics **100**, 1290–1296 (1994).

[23] R.C. Morrison Q. Zhao and R.G. Parr, "From electron densities to kohn-sham kinetic energies, orbital energies, exchange-correlation potentials, and exchange-correlation energies," Phys. Rev. A **50**, 2138 (1994).

[24] Oleg V. Gritsenko, Robert van Leeuwen, and Evert Jan Baerends, "Molecular kohn-sham exchange-correlation potential from the correlated *ab initio* electron density," Phys. Rev. A **52**, 1870–1874 (1995).

[25] Claudia Filippi, Xavier Gonze, and C. J. Umrigar, *Recent Developments and Applications of Density Functional Theory*, edited by J. M. Seminario (Elsevier, Amsterdam, 1996) pp. 295–326.

[26] Robert Leeuwen, Oleg V. Gritsenko, and Evert Jan Baerends, "Analysis and modelling of atomic and molecular kohn-sham potentials," in *Density Functional Theory I*, Topics in Current Chemistry, Vol. 180, edited by R.F. Nalewajski (Springer Berlin Heidelberg, 1996) pp. 107–167.

[27] O.V. Gritsenko and E.J. Baerends, "Effect of molecular dissociation on the exchange-correlation kohn-sham potential," Phys.Rev. A **54**, 1957 (1996).

[28] Lucas O. Wagner, E.M. Stoudenmire, Kieron Burke, and Steven R. White, "Reference electronic structure calculations in one dimension," Phys. Chem. Chem. Phys. **14**, 8581 – 8590 (2012).

[29] M. Thiele, E. K. U. Gross, and S. Kümmel, "Adiabatic approximation in nonperturbative time-dependent density-functional theory," Phys. Rev. Lett. **100**, 153004 (2008).

[30] Claudio Verdozzi, "Time-dependent density-functional theory and strongly correlated systems: Insight from numerical studies," Phys. Rev. Lett. **101**, 166401 (2008).

[31] Steven R. White, "Density matrix formulation for quan-

tum renormalization groups," Phys. Rev. Lett. **69**, 2863 (1992).

[32] Steven R. White, "Density-matrix algorithms for quantum renormalization groups," Phys. Rev. B **48**, 10345 (1993).

[33] U. Schollwöck, "The density-matrix renormalization group," Rev. Mod. Phys. **77**, 259–315 (2005).

[34] Eric Cancès and Claude Le Bris, "On the convergence of scf algorithms for the hartree-fock equations," ESAIM: Mathematical Modelling and Numerical Analysis **34**, 749–774 (2000).

[35] Eric Cancs, in *Mathematical Models and Methods for Ab Initio Quantum Chemistry* (Springer, Berlin, 2007).

[36] A. Szabo and N. S. Ostlund, *Modern Quantum Chemistry* (Dover Publishing, Mineola, New York, 1996).

[37] Cyrus J. Umrigar and M.P. Nightingale, *Quantum Monte Carlo Methods in Physics and Chemistry*, Vol. 525 (Springer, 1999).

[38] H. Englisch and R. Englisch, "Hohenberg-Kohn theorem and non-V-representable densities," Physica A: Statistical Mechanics and its Applications **121**, 253 – 268 (1983).

[39] Mel Levy, "Electron densities in search of hamiltonians," Phys. Rev. A **26**, 1200–1208 (1982).

[40] In this paper we utilize the pure-state formulation of DFT. To generalize, a ground-state ensemble and trace replace $\Psi[n]$ and its expectation value in Eq. (4) [7].

[41] Robert van Leeuwen, "Density functional approach to the many-body problem: Key concepts and exact functionals," (Academic Press, 2003) pp. 25 – 94.

[42] Andreas Görling, "Kohn-sham potentials and wave functions from electron densities," Phys. Rev. A **46**, 3753–3757 (1992).

[43] Yue Wang and Robert G. Parr, "Construction of exact kohn-sham orbitals from a given electron density," Phys. Rev. A **47**, R1591–R1593 (1993).

[44] P. R. T. Schipper, O. V. Gritsenko, and E. J. Baerends, "Kohn-sham potentials corresponding to slater and gaussian basis set densities," Theoretical Chemistry Accounts: Theory, Computation, and Modeling (Theoretica Chimica Acta) **98**, 16–24 (1997), 10.1007/s002140050273.

[45] K. Peirs, D. Van Neck, and M. Waroquier, "Algorithm to derive exact exchange-correlation potentials from correlated densities in atoms," Phys. Rev. A **67**, 012505 (2003).

[46] Kieron Burke and Lucas O. Wagner, "Dft in a nutshell," Int. J. Quant. Chem. (2012), 10.1002/qua.24259.

[47] R. M. Dreizler and E. K. U. Gross, *Density Functional Theory: An Approach to the Quantum Many-Body Problem* (Springer–Verlag, Berlin, 1990).

[48] Oleg V. Gritsenko, Robert van Leeuwen, and Evert Jan Baerends, "Molecular kohn-sham exchange-correlation potential from the correlated *ab initio* electron density," Phys. Rev. A **52**, 1870–1874 (1995).

[49] William H. Press, Saul A. Teukolsky, William T. Vetterling, and Brian P. Flannery, eds., *Numerical Recipes*, 3rd ed. (Cambridge University Press, New York, 2007).

[50] E. M. Stoudenmire, Lucas O. Wagner, Steven R. White, and Kieron Burke, "One-dimensional continuum electronic structure with the density-matrix renormalization group and its implications for density-functional theory," Phys. Rev. Lett. **109**, 056402 (2012).

[51] J. H. Eberly, Q. Su, and J. Javanainen, "High-order harmonic production in multiphoton ionization," J. Opt. Soc. Am. B **6**, 1289–1298 (1989).

[52] N. Helbig, J. I. Fuks, M. Casula, M. J. Verstraete, M. A. L. Marques, I. V. Tokatly, and A. Rubio, "Density functional theory beyond the linear regime: Validating an adiabatic local density approximation," Phys. Rev. A **83**, 032503 (2011).

[53] The density shown in Fig. 2 is given by $\tilde{n}(x) = e^{x/15 - x^2/2 + x^4/20 - x^6/750}$, divided by a normalization factor such that it contains four electrons.

[54] W. Kohn, "v-representability and density functional theory," Phys. Rev. Lett. **51**, 1596–1598 (1983).

[55] C.G. Broyden, "A class of methods for solving nonlinear simultaneous equations," Mathematics of Computation **19**, 577–593 (1965).

[56] Steven M. Valone, "A one-to-one mapping between one-particle densities and some n-particle ensembles," The Journal of Chemical Physics **73**, 4653–4655 (1980).

[57] V. R. Saunders and I. H. Hillier, "A "levelshifting" method for converging closed shell hartree–fock wave functions," International Journal of Quantum Chemistry **7**, 699–705 (1973).

[58] Andrew D. Daniels and Gustavo E. Scuseria, "Converging difficult scf cases with conjugate gradient density matrix search," Phys. Chem. Chem. Phys. **2**, 2173–2176 (2000).

[59] Konstantin N. Kudin, Gustavo E. Scuseria, and Eric Cancs, "A black-box self-consistent field convergence algorithm: One step closer," The Journal of Chemical Physics **116** (2002).

[60] Lea Thogersen, Jeppe Olsen, Danny Yeager, Poul Jorgensen, Pawel Salek, and Trygve Helgaker, "The trust-region self-consistent field method: Towards a black-box optimization in hartree–fock and kohn–sham theories," The Journal of Chemical Physics **121**, 16–27 (2004).

[61] Juliano B. Francisco, Jose Mario Martinez, and Leandro Martinez, "Globally convergent trust-region methods for self-consistent field electronic structure calculations," The Journal of Chemical Physics **121**, 10863–10878 (2004).

[62] C. Yang, J. Meza, and L. Wang, "A trust region direct constrained minimization algorithm for the kohnsham equation," SIAM Journal on Scientific Computing **29**, 1854–1875 (2007), http://epubs.siam.org/doi/pdf/10.1137/060661442.

[63] John P. Perdew and Mel Levy, "Extrema of the density functional for the energy: Excited states from the ground-state theory," Phys. Rev. B **31**, 6264–6272 (1985).

[64] J.P. Perdew, "What do the kohn-sham orbitals mean? how do atoms dissociate?" in *Density Functional Methods in Physics*, edited by R.M. Dreizler and J. da Providencia (Plenum, NY, 1985) p. 265.

[65] Marten A. Buijse, Evert Jan Baerends, and Jaap G. Snijders, "Analysis of correlation in terms of exact local potentials: Applications to two-electron systems," Phys. Rev. A **40**, 4190–4202 (1989).

[66] N. Helbig, I. V. Tokatly, and A. Rubio, "Exact kohn–sham potential of strongly correlated finite systems," J. Chem. Phys. **131**, 224105 (2009).

[67] David G. Tempel, Todd J. Martínez, and Neepa T. Maitra, "Revisiting molecular dissociation in density functional theory: A simple model," Journal of Chemical Theory and Computation **5**, 770–780 (2009).

[68] M. Fuchs, Y.-M. Niquet, X. Gonze, and K. Burke, "Describing static correlation in bond dissociation by kohn–sham density functional theory," The Journal of Chemical Physics **122**, 094116 (2005).

[69] Oleg Gritsenko and Evert Jan Baerends, "Correct dissociation limit for the exchange-correlation energy and potential," International Journal of Quantum Chemistry **106**, 3167–3177 (2006).

[70] J. C. Slater, "The theory of complex spectra," Phys. Rev. **34**, 1293–1322 (1929).

[71] Larry Armijo, "Minimization of functions having lipschitz continuous first partial derivatives," Pacific J. Math. **16**, 1–3 (1966).

[72] Carsten A. Ullrich, *Time-Dependent Density-Functional Theory* (Oxford University Press, Oxford, 2012).

[73] M. Thiele and S. Kümmel, "Frequency dependence of the exact exchange-correlation kernel of time-dependent density-functional theory," Phys. Rev. Lett. **112**, 083001 (2014).

[74] Paola Gori-Giorgi and Michael Seidl, "Density functional theory for strongly-interacting electrons: perspectives for physics and chemistry," Phys. Chem. Chem. Phys. **12**, 14405–14419 (2010).

[75] Angela D. Rabuck and Gustavo E. Scuseria, "Improving self-consistent field convergence by varying occupation numbers," The Journal of Chemical Physics **110**, 695–700 (1999).

[76] Aron J. Cohen and Paula Mori-Sánchez, "Dramatic changes in electronic structure revealed by fractionally charged nuclei," arXiv:1308.1991 (2013).

[77] Neepa T. Maitra, "Undoing static correlation: Long-range charge transfer in time-dependent density-functional theory," The Journal of Chemical Physics **122**, 234104 (2005).

[78] Mario A. Natiello and Gustavo E. Scuseria, "Convergence properties of hartreefock scf molecular calculations," International Journal of Quantum Chemistry **26**, 1039–1049 (1984).

[79] I DAmico, JP Coe, VV Franca, and K Capelle, "Quantum mechanics in metric space: wave functions and their densities," Physical Review Letters **106**, 050401 (2011).

[80] M.A. Maroun, *Generalized Quantum Theory and Mathematical Foundations of Quantum Field Theory* (University of California, Riverside, 2013) p. 69.

[81] U. von Barth and L. Hedin, "A local exchange-correlation potential for the spin polarized case," Journal of Physics C: Solid State Physics **5**, 1629 (1972).

[82] L. Wilk S. H. Vosko and M. Nusair, "Accurate spin-dependent electron liquid correlation energies for local spin density calculations: a critical analysis," Can. J. Phys. **58**, 1200–1211 (1980).

[83] C.A. Coulson and I. Fischer, "Xxxiv. notes on the molecular orbital treatment of the hydrogen molecule," Philosophical Magazine Series 7 **40**, 386–393 (1949).

[84] John P. Perdew, Andreas Savin, and Kieron Burke, "Escaping the symmetry dilemma through a pair-density interpretation of spin-density functional theory," Phys. Rev. A **51**, 4531–4541 (1995).

[85] Rudiger Bauernschmitt and Reinhart Ahlrichs, "Stability analysis for solutions of the closed shell kohn–sham equation," The Journal of Chemical Physics **104**, 9047–9052 (1996).

[86] O. V. Gritsenko and E. J. Baerends, "The spin-unrestricted molecular kohn–sham solution and the analogue of koopmans's theorem for open-shell molecules," The Journal of Chemical Physics **120**, 8364–8372 (2004).

[87] C. A. Ullrich and W. Kohn, "Kohn-sham theory for ground-state ensembles," Phys. Rev. Lett. **87**, 093001 (2001).

[88] J.T. Chayes, L. Chayes, and MaryBeth Ruskai, "Density functional approach to quantum lattice systems," Journal of Statistical Physics **38**, 497–518 (1985).